
SCREAM 3.0: Super-elastic Continuum Robot for Endoscopic Articulation and Manipulation

Major Qualifying Project

Submitted By:

PHILLIP ABELL, ROBOTICS ENGINEERING
SAMUEL JOHNSON, ROBOTICS ENGINEERING
SABRINA LIU, ROBOTICS ENGINEERING
ZHONGCHUAN XU, ROBOTICS ENGINEERING

Project Advisors:

PROF. LORIS FICHERA
PROF. YUXIANG LIU



WORCESTER POLYTECHNIC INSTITUTE

AUG 2020 - MAY 2021

This report represents the work of four WPI undergraduate students submitted to the faculty as evidence of completion of a degree requirement. WPI routinely publishes these reports on the web without editorial or peer review.

ABSTRACT

The objective of this project is to design and build an at-scale continuum robot to enhance a physician's dexterity in minimally invasive endoscopic surgery to treat laryngeal tumors. Laryngeal tumors are common, yet challenging to treat endoscopically due to the lack of articulation in commercially available surgical instruments. Teaming up with a physician at Brigham and Women's Hospital, we designed and constructed an integrated device with a needle-sized, steerable laser sheath to make formerly untreatable tumors accessible and operable. We also present the design and construction of an actuation unit capable of providing three degrees of freedom: rotation, translation, and distal tip bending. The system encompasses a steerable sheath, control panel, and actuation module that directly integrates with the endoscopic handle currently being used by physicians.

EXECUTIVE SUMMARY

Laryngeal tumors affect 1 in 40 adults worldwide, resulting in issues with speech and breathing [1]. The traditional treatment approach for these vocal fold tumors is an inpatient surgical procedure requiring general anesthesia, which is time-consuming and expensive for both physicians and patients [2]. A more economical and convenient alternative is an office-based procedure that uses laser pulses to treat laryngeal tumors endoscopically. On average, an office-based laser surgery is \$5000 cheaper than a traditional surgery [3, 4]. The patient remains fully awake and only local anesthesia is needed, lowering complication rates. The procedure takes about five minutes, and the patient can walk out of the office with little impact on the rest of their day [2, 5].

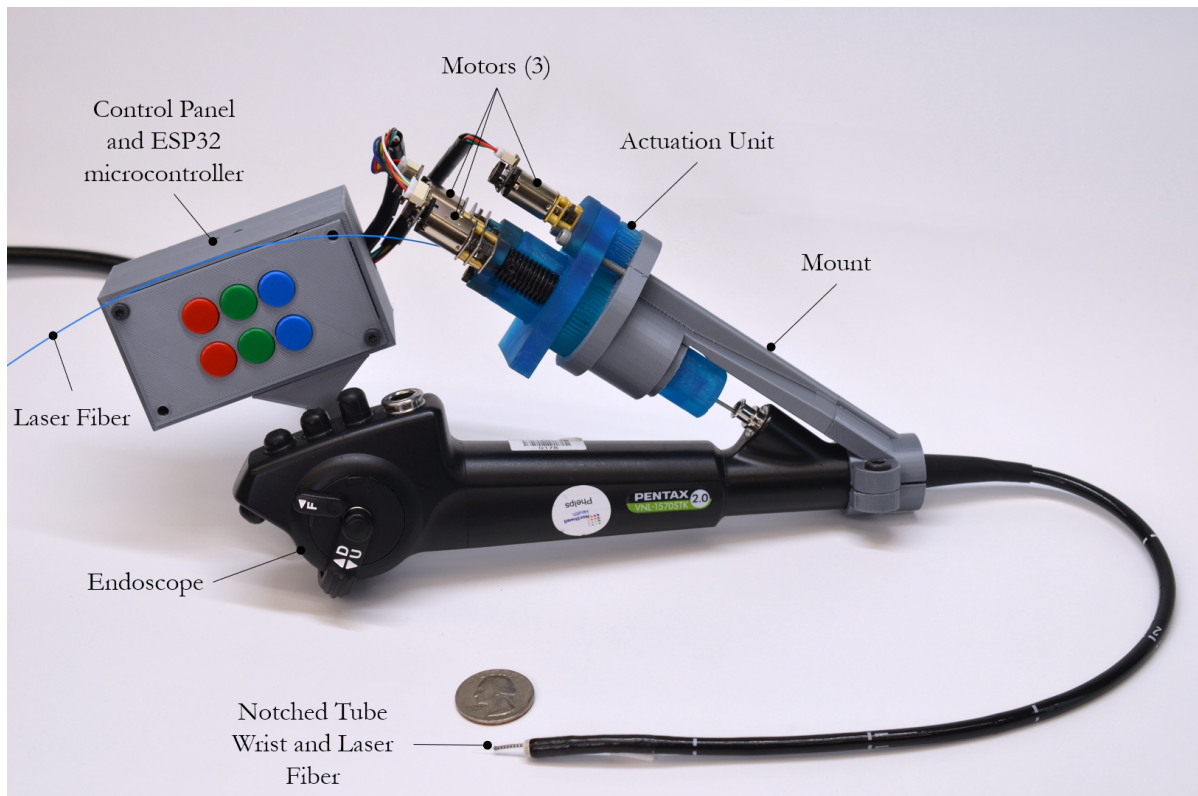


Figure 1: Proposed robot for office-based laser surgery of the vocal folds. The robot can be mounted on an endoscope, and it can be controlled by the operating physician using the same hand he/she uses to hold the scope.

In the current setup for in-office laser laryngeal treatment, a laser fiber is passed through the working channel of an endoscope. The endoscope's flexible tube is passed into the patient's nose down to the throat. A small chip-tip camera enables the physician to see where laser pulses are applied.

Despite its many benefits, office-based surgery is still underutilized because the endoscopic device currently used for such in-office procedures has significant limitations. Certain areas of the vocal folds cannot be treated at all due to the articulation capabilities of the endoscope. Patients with such tumors must undergo traditional surgery. The endoscope is mechanically unable to undergo the significant bending required to reach tumors on the underside of the right vocal fold and other locations. Furthermore, aiming the endoscope to ensure that laser pulses successfully treat the tumor is a difficult and disorienting task, since the camera and laser fiber are fixed together. Therefore, we propose a robotic system that would enable the physician to steer the laser fiber independently of the endoscopic tube, which would also expand the treatable surface area in the vocal folds.

One major constraint for such a robotic system is the size of the endoscope's working channel. With a less than 2 mm diameter opening, a traditional joint-and-link robotic system is not a viable option. Instead, we propose the use of a continuum link robot to enable steering of the laser fiber, which has been manufactured on the millimeter scale [6]. A continuum link robot provides distal articulation by means of a tube with asymmetric notches.

Little work has been done in creating an integrated, at-scale system ready for clinical trials. In this project, we aim to design, prototype, and validate a fully integrated, robotic steerable laser system that enables controlling the laser fiber tip in three degrees of freedom: rotation, translation, and bending. One of the main challenges of this undertaking is the complexity of creating an integrated device with so many pieces each presenting their own unique challenges. Our solution encompasses several components which all needed to come together to create a successful device, as shown in Fig. 1.

To enable distal tip bending, we first conducted simulations in MATLAB to select the proper geometry for our custom-cut Nitinol steerable sheaths. The four steerable sheath geometries that enabled the highest visualized surface area in our larynx models were selected to be manufactured (See Section 2.2).

Preliminary tests with the laser fiber in a Nitinol steerable sheath showed that the laser fiber currently used in office-based laser surgery (Endostat laser fiber) prevents the notched tube from curving properly and bending completely. Therefore, we conducted an experiment to assess thinner laser fiber candidates and selected a 200 micron laser fiber instead. According to our experiments, the 200 micron laser fiber required a lower amount of force to bend compared to the Endostat laser fiber, and it did not interfere with the bending of the steerable sheath (See Section 2.3). In order to center the laser fiber inside the Nitinol steerable sheath and to affix the tendon to the tip of the steerable sheath, we designed and manufactured a tiny end cap measuring 1.1

mm in diameter (See Section 2.5).

We also needed to find a suitable solution to connect the Nitinol steerable sheath to the actuation unit. The tubing would need to be axially flexible to accommodate the patient's anatomical bends as it passed through the endoscope's flexible working shaft, but also torsionally rigid so that we could transmit rotational forces from the actuation unit to the laser fiber. Friction inside the working channel was also a major concern. We decided to use spring coils, which are used in other commercially available endoscopic surgical instruments. We tested five candidates and selected the two which had the highest rotational transmission ratio from end to end inside the working channel of the endoscope (See Section 2.4).

The actuation unit is the component of the device which encompasses the motors and gears needed to manipulate the steerable sheath at the end of the endoscope (See Fig. 1 and Section 2.6). This unit needs to be able to translate the steerable sheath linearly, rotate the steerable sheath, and flex the steerable sheath. The design goal of the actuation unit is to have a highly compact device that has these three degrees of freedom. Taking inspiration from a design recently published in the biomedical literature [7], we created a new design where the optical fiber is threaded through a hollow lead screw. The final design is a 2.5 cm diameter cylinder with a 10cm height and weights only at around 100 g total. Fig. 2 shows how the actuation unit achieves control of three degrees of freedom.

The lead screw is attached to the tube and translated linearly through the rotation of the lead screw nut. With the transmission system, the linear action of the actuation unit can be driven by a motor that is placed on the rear of the actuation unit using a connection shaft. In order to flex the steerable sheath, the tendon is attached to both the steerable sheath and a winch, which is actuated by a worm gear. The rotation of the winch pulls and releases the tendon depending on the direction of rotation, flexing the steerable sheath. Lastly, a gear encases the outside of the housing and meshes with a smaller gear attached to a motor. This allows the gear to rotate the entire actuation unit, thereby rotating the laser fiber. These three degrees of freedom are summarized in Fig. 2.

The laser fiber and spring coil is attached to the hollow lead screw using adhesives, so that the laser fiber can translate linearly and rotate along with the lead screw. The tendon is passed through the hollow center of the lead screw and attached to the tendon winch. The design has the advantage of being small and lightweight. However, linear translation of the hollow lead screw bends the steerable sheath, because the tendon is fixed to a winch located behind the lead screw, which does not advance as the lead screw does.

To control the actuation unit, our team envisioned a clip-on device to the endoscope that would enable the physician to control both the endoscope and steerable laser with their right hand. This solution would also enable us to simplify our device and minimize complexity by combining the actuation unit and its controller (See Section 2.7).

The control panel is made up of six buttons, an ESP32 microcontroller, and two L293D dual

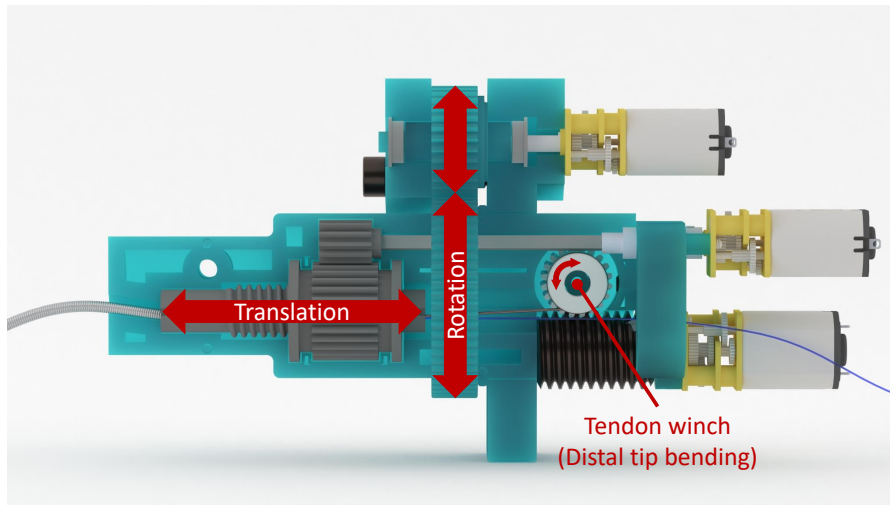


Figure 2: The actuation unit enables 3-DOF control of the laser fiber: translation, rotation, and distal tip bending.

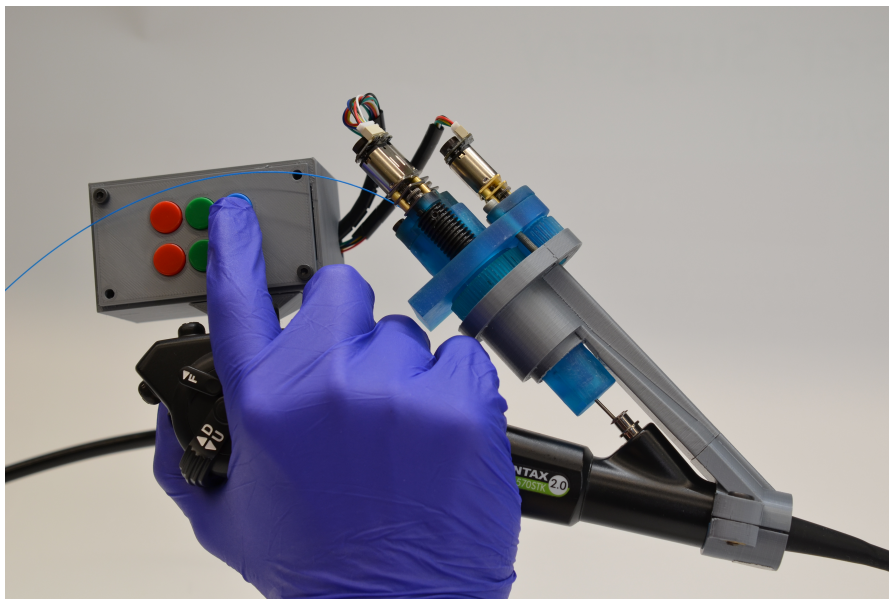


Figure 3: Integrated device, mounted onto endoscope. A hand models how physicians would be able to manipulate the device.

H-Bridges. The buttons are separated in to 3 pairs with each pair controlling a degree of freedom for the steerable sheath, either translation, rotation or bending. The ESP32 handles the user inputs from the buttons and controls the corresponding motors in their proper direction. This control panel, along with the ESP32, is housed in a small box that can also directly be mounted onto the endoscope handle. Power is currently supplied by a bench-top power supply. This setup enables the physician to control the entire actuation unit with just one hand, as shown in Fig. 3.

During testing, we verified that our device met three out of four of our design goals. The

steerable sheath in our design has a 1.1 mm outer diameter, and along with the spring coil tubing, fits into the 2 mm working channel of the endoscope. We are able to continuously rotate the laser fiber, satisfying our design requirement of enabling 360 degrees of rotation. We are also able to translate the laser fiber 14 mm, which meets our design goal of being able to translate the laser fiber 1-2 cm. Lastly, we were able to bend the laser fiber 80 degrees, which falls slightly short of our goal of 90 degrees. However, we are able to bend the laser fiber in a very tight radius. The four steerable sheath designs we manufactured are able to bend in radii ranging from 3 mm to 13 mm. The geometry used in testing was 10 mm long with a 3 mm bending radius. It is possible that the laser fiber is unable to accommodate bending in such a tight radius.

Our work this year produced a prototype that is ready to be tested by laryngologists in cadavers. One day, a version of this device will enable physicians to treat more patients in a shorter amount of time, and treat patients who were previously considered untreatable in the office.

ACKNOWLEDGEMENTS

This work was supported by Worcester Polytechnic Institute and the Cognitive Medical Technology and Robotics Laboratory (COMET Lab). Funding was provided by the NIH (National Institutes of Health).

We would like to thank all of our advisors for their guidance and expertise, especially Professor Fichera for being a very involved advisor and holding us to a high standard. Thank you to Professor Liu for providing expertise with laser fibers, a crucial component of our device. Many thanks to Dr. Thomas L. Carroll for making himself available for testing prototypes and providing expert feedback. We would also like to thank Alex Chiluisa for helping us run all of the experiments this year. Thank you to Dr. Peter York for helping to manufacture the end caps for our device.

TABLE OF CONTENTS

Acknowledgements	vii
	Page
List of Tables	x
List of Figures	xi
1 Introduction	1
2 Design, Prototyping, Manufacturing, and Integration	4
2.1 Gathering of Requirements	4
2.2 Steerable Sheath Design	5
2.3 Selection of the Laser Fiber	8
2.4 Spring Coil	10
2.5 End Effector Cap	14
2.6 Actuation Unit	14
2.7 Controller	18
3 Integration and Testing	21
3.1 Integration	21
3.2 Mechanical Design Evaluation	22
3.2.1 Steerable Sheath Bending	23
3.2.2 Translation	25
3.2.3 Rotation	27
3.3 ENT User Study	28
4 Discussion and Future Work	29
4.1 Advancement Over SCREAM 2.0	29
4.2 Future Work	30
4.2.1 User Study	30
4.2.2 Actuation Unit	30
4.2.3 Controller	31

4.2.4	Materials and Sanitation	31
4.2.5	Steerable Sheath	31
4.3	Conclusion	32
	Bibliography	33
	A Appendix A: Authorship	35
	B Appendix B: Wiring Diagram for Control Panel	37
	C Appendix C: Experimental Protocol for ENT User Study	39
C.1	Overview	39
C.2	Experiment	39

LIST OF TABLES

TABLE	Page
2.1 Summary of simulation results of all tested sheaths. L is steerable length and R is the minimum bending radius. The table shows the simulation result of each sheath configuration as the total visible area.	8
2.2 Ratio of rotation transmitted in each direction of rotation, under Case 1: tip bent at 0 degrees.	14

LIST OF FIGURES

1	Proposed robot for office-based laser surgery of the vocal folds. The robot can be mounted on an endoscope, and it can be controlled by the operating physician using the same hand he/she uses to hold the scope.	ii
2	The actuation unit enables 3-DOF control of the laser fiber: translation, rotation, and distal tip bending.	v
3	Integrated device, mounted onto endoscope. A hand models how physicians would be able to manipulate the device.	v

FIGURE		Page
---------------	--	-------------

1.1	Current procedure for removing laryngeal tumors using a laser fiber passed through an endoscope. The endoscope is passed through the patient’s nose down to their larynx. The physician can see a live video feed from the endoscope’s chip-tip camera. Reproduced from [8].	2
1.2	Frontal cut of the larynx: (a) The area highlighted in blue shows the endoscope’s field of view; (b) Reaching tumors located in areas that require significant bending can result in the endoscope’s field of view being completely blocked by tissue. Reproduced from [9].	3
2.1	View of endoscope’s distal end, showing its chip-tip camera and 2 mm diameter working channel.	5
2.2	View from the top of one of the larynx models used in simulation. Tissue visibility of the currently used system. As stated, the current system uses a non-steerable laser fiber. This image illustrates how the straight laser fiber is unable to treat the right side of the larynx. There is a distinct strip of non-treatable, tissue in the model. We suspect this is a combination of mechanical constraints of how the physician is able to move their steerable sheath, and the geometry of the endoscope.	6
2.3	Visualisation of steerable sheath parameters. L is the steerable length. This is measured from the bottom of the lowermost notch to the top of the uppermost notch along the spine of the sheath. The spine is the neutral bending plane that runs through the uncut section of the sheath. It does not become stretched nor compressed. R is the minimum bending radius of the arc formed by the sheath when all notches are closed.	7

LIST OF FIGURES

2.4 Comparison between steerable (right column) and non-steerable (left column) laser fiber. The top row is for the first larynx model and the second row is the second model. This comparison shows that the steerable laser fiber is able to reach significantly more tissue consistently across different larynges. The particular sheath configuration used to produce this result is $L = 10mm; R = 3mm$ 9

2.5 Experimental setup used to test the force required to bend the Nitinol sheath with under 4 conditions: with an empty lumen, with a 105 micron laser fiber, with a 200 micron laser fiber, and with the Endostat laser fiber. 10

2.6 Graph showing amount of force exerted by the tendon, in N, as it is displaced to gradually bend the Nitinol sheath under different conditions: open sheath (no laser fiber), with a 105 micron laser fiber, with a 200 micron laser fiber, and with the conventionally used Endostat laser fiber. The Endostat laser fiber requires significantly more force to bend and does not allow the steerable sheath to close completely. Therefore, we elect to use the 200 micron laser fiber instead, which require comparably lower amounts of force to bend while inside the steerable sheath. 11

2.7 Experimental setup for spring coil rotation tests to determine the ratio of rotation transmitted by 5 spring coil candidates. 13

2.8 Three tip angles used for testing spring coil candidates for ratio of rotation transmitted in both directions (CW and CCW): A) 0, B) 60, and C) 90 degrees. 13

2.9 Steerable sheath shown fully bent with laser fiber tangentially following the outer arc of the steerable sheath’s curvature, not aligned with the centerline of the steerable sheath, which the Nitinol tendon is parallel to. 15

2.10 End cap design. Two holes are for the Nitinol tendon to be attached through, and the hole in the center is for centering the laser fiber in the steerable sheath so that it follows the centerline of the bending steerable sheath’s curvature. 16

2.11 Exploded render of actuation unit showing main components. 16

2.12 Side view of the actuation unit opened to show internal components. The lead screw enables translation of the laser fiber, two gears on the outside of the actuation unit enable rotation, and a tendon winch enables bending of the steerable sheath and laser fiber. 17

2.13 Existing office-based laser surgery setup. Both of the physician’s hands are occupied. Reproduced from [8]. 18

2.14 Custom-made button panel to control three degrees of freedom using the actuation unit to control the laser fiber. Designed to be mounted in a box directly onto the endoscope, enabling one-handed control of the actuation unit. 19

3.1 End cap design integrated with Nitinol steerable sheath, laser fiber, and tendon. . . 22

3.2 Fully integrated device, showing the button panel and actuation unit mounted on top of an endoscope that is currently used in office-based laser surgery of laryngeal tumors. 23

3.3	Test setup used for verification testing of the device.	24
3.4	Camera and testing area setup for verification testing.	25
3.5	Stages of bending the steerable sheath from straight to fully bent, with the laser fiber inside the steerable sheath.	26
3.6	Full bending of the steerable sheath to 80 degrees. Created using online protractor tool [10].	26
3.7	Stages of full translation using the device. In this trial, the device translates the steerable sheath 13.5 mm. The starting and end points are measured from the tip of the laser fiber since the tip of the steerable sheath is not initially visible.	27
3.8	Sequence of full rotations using the device. The laser fiber and steerable sheath are at their fully bent position so that the laser fiber can be used to mark the rotation of the steerable sheath.	28
4.1	Progression of design across the past 3 years of SCREAM.	30
B.1	Wiring diagram for button panel, H-bridges, and motors.	38

INTRODUCTION

Laryngeal tumors affect 1 in 40 adults worldwide, resulting in issues with speech and breathing [1]. The traditional treatment approach for these tumors is an inpatient surgical procedure requiring general anesthesia, which is time-consuming and expensive for both physicians and patients [2]. In particular, patients with rapid recurrent papillomatosis (RRP) suffer significant financial burden and impact on their lives. Two out of every 100,000 adults and four out of every 100,000 children suffer from RRP. Patients with RRP repeatedly develop new tumors in their larynx and require multiple surgeries to remove these tumors. About 20% of RRP patients require more than 4 surgeries per year [11]. There is no known cure for RRP.

A more economical and convenient alternative is an office-based procedure that uses laser pulses to treat laryngeal tumors endoscopically. On average, an office-based laser surgery is \$5000 less expensive than a traditional surgery [3, 4]. The patient remains fully awake and only local anesthesia is needed, lowering complication rates. The procedure takes about five minutes, and the patient can walk out of the office with little impact on the rest of their day [2, 5]. The current setup for in-office laser laryngeal treatment is depicted in Fig. 1.1. A laser fiber is passed through the working channel of an endoscope. The endoscope's flexible shaft is passed into the patient's nose down to the throat. A small chip-tip camera enables the physician to see where laser pulses are applied.

Unfortunately, office-based procedures are still underutilized because the endoscopic device currently used for such in-office procedures has significant limitations. First, certain areas of the vocal folds cannot be treated at all due to the articulation capabilities of the endoscope. For example, tumors located on the underside of the right vocal fold are considered untreatable, and patients with such tumors must undergo traditional surgery. Right-handed surgeons have difficulty rotating the endoscope to an orientation where they can both see and treat tumors located on the right vocal fold. The endoscope is mechanically unable to undergo the significant



Figure 1.1: *Current procedure for removing laryngeal tumors using a laser fiber passed through an endoscope. The endoscope is passed through the patient's nose down to their larynx. The physician can see a live video feed from the endoscope's chip-tip camera. Reproduced from [8].*

bending required to reach tumors on the right vocal fold and other locations. Furthermore, aiming the endoscope to ensure that laser pulses successfully treat the tumor is a difficult and disorienting task. The physician cannot aim the laser fiber without moving the camera and changing their field of view, since the camera and laser fiber are fixed together (Fig. 1.2). In some cases, such as where significant bending is required, aiming the laser fiber results in the camera becoming completely obscured by tissue. Therefore, we propose a robotic system that would enable the physician to steer the laser fiber independently of the endoscopic shaft, which would also expand the treatable surface area in the vocal folds.

One major constraint for such a robotic system is the size of the endoscope's working channel. With a less than a 2 mm diameter opening, a traditional joint-and-link robotic system is not a viable option. Instead, we propose the use of a continuum robot to enable steering of the laser fiber, which has been manufactured on the millimeter scale [6]. A continuum robot provides distal articulation by means of a tube with asymmetric notches. Since the tube has a hollow lumen, the laser fiber can be passed through and articulated using this tube or steerable sheath. A wire is fixed to the end of this tube, and acts similar to a tendon bending a wrist – pulling on this tendon wire results in distal articulation, or a curving motion of the notched tube. We also take inspiration from recent robotics literature for the development of a compact actuation unit to fully control and motorize the system. The actuation unit controls the bending, rotation, and translation of the steerable laser fiber.

This project builds on the work done by two past project teams, SCREAM 1 and SCREAM 2, who in the past two years have validated the feasibility of creating a miniaturized continuum robotic system and created a motorized prototype [6, 9]. We extend the work in these prior projects by creating an integrated, at-scale system ready for clinical trials. In this project, we aim

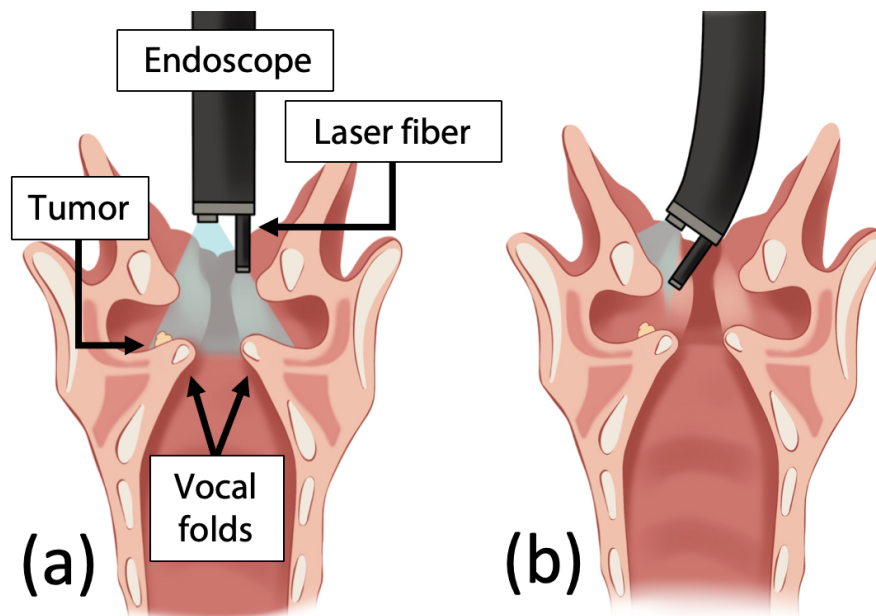


Figure 1.2: *Frontal cut of the larynx: (a) The area highlighted in blue shows the endoscope’s field of view; (b) Reaching tumors located in areas that require significant bending can result in the endoscope’s field of view being completely blocked by tissue. Reproduced from [9].*

to design, prototype, and validate a fully integrated, robotic steerable laser system. The main components of the project include a compact actuation unit capable of delivering three degrees of freedom (distal bending, translation, and rotation) and integrating directly into the current workflow and an accompanying controller.

Paper Outline This paper documents our journey from idea to prototype, and from design to testing. The contents are as follows. **Design, Prototyping, and Manufacture** describes the process of designing and acquiring the different parts of the system, as well as the integration of all of the parts. **Testing and Validation** details how the integrated system was evaluated. **Discussion and Future Work** outline suggestions for future iterations of this project.

DESIGN, PROTOTYPING, MANUFACTURING, AND INTEGRATION

2.1 Gathering of Requirements

Iterations of this project have partnered with a laryngologist who uses office-based procedures to treat tumors of the vocal chords. Based on interviews with him, information available to us from the previous two project teams, and background research, we have determined the following functional constraints and requirements. The device we create shall:

- Be smaller than 2 mm in diameter to fit into the working channel for the endoscope (see Fig. 2.1 for reference).
- Be able to bend the tip of the laser fiber 90 degrees in a radius smaller than 14 mm, the radius at which the endoscope tip currently bends.
- Be able to rotate the laser fiber 360 degrees.
- Be able to translate the laser fiber approximately 1-2 cm, in and out of the endoscope working channel.

We also identified the following non-functional requirements:

- The need to integrate a robotic system with the existing endoscope handle in a way that is intuitive and easy for the physician to operate.
- Controls that enable one physician to complete the procedure alone.

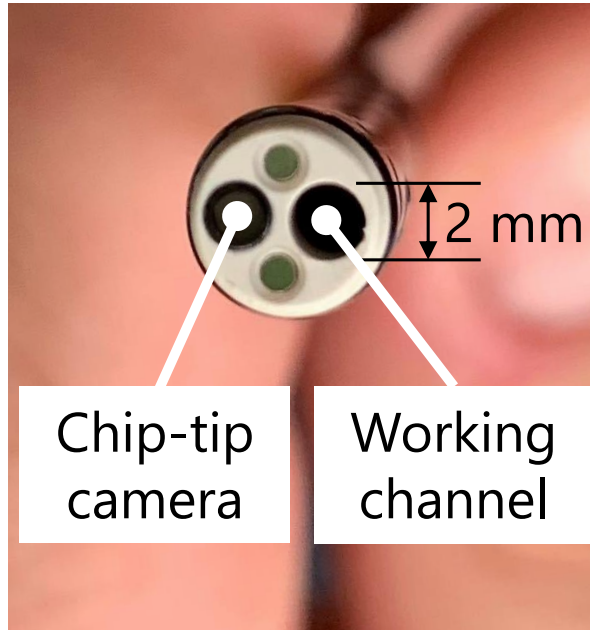


Figure 2.1: View of endoscope's distal end, showing its chip-tip camera and 2 mm diameter working channel.

2.2 Steerable Sheath Design

One of the main motivations behind using an articulated steerable sheath is to eliminate unreachable space within the larynx. The current methods and tools available for office-based laryngeal laser surgery create a segment of unreachable space on the right side of the larynx. This issue was recently investigated by Chan et al. [12]. Through simulation studies, their team found that limitations in the range of motion attainable by the endoscope and optical fiber make it hard for physicians to certain areas within the larynx. Here, we use the same simulation software developed in [12] to understand the benefit of introducing steering optical fibers in office-based vocal folds surgery. This gives us the freedom to try as many sheath geometries without having to actually fabricate them. Briefly, in these simulations we deploy an endoscope and steering optical fiber within a 3D model of the human larynx. Then we generate a large number (10,000) of reachable instrument poses using a motion planning algorithm (Rapidly-Expanding Random Trees). For each of these poses, the simulation determined if the robot collided with the larynx. Finally, a ray-casting algorithm was used to determine what regions of the larynx would be treatable by the laser.

Fig. 2.2 shows the result of this simulation and highlights the unreachable space along the right side of the larynx when a conventional non-steering optical fiber is used. We hypothesized that a steerable laser fiber would improve the treatability by providing coverage of the entire larynx and vocal folds. Past studies have demonstrated the feasibility of constructing miniaturized notched tubes from Nickel-titanium (NiTi or Nitinol) alloy [13, 6]. Nitinol is an optimal material

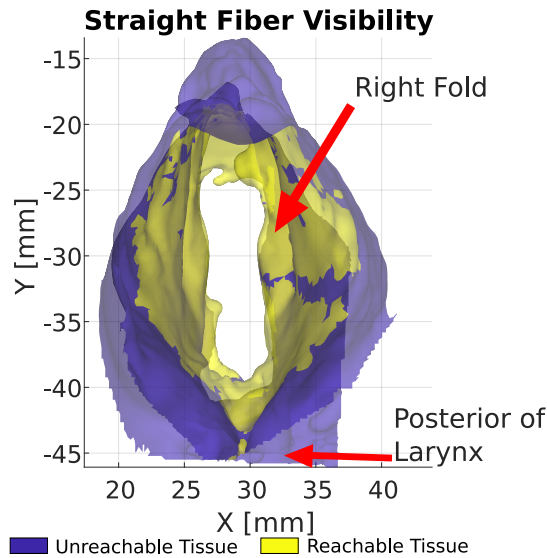


Figure 2.2: View from the top of one of the larynx models used in simulation. Tissue visibility of the currently used system. As stated, the current system uses a non-steerable laser fiber. This image illustrates how the straight laser fiber is unable to treat the right side of the larynx. There is a distinct strip of non-treatable, tissue in the model. We suspect this is a combination of mechanical constraints of how the physician is able to move their steerable sheath, and the geometry of the endoscope.

for this application because of its super-elastic properties, which allows it to keep its original shape despite repeated bending. After the tendon pull-wire is released, the Nitinol notched tube will return to its original shape. The manufacturing process involves removing small notches from the Nitinol tube and attaching a pull-wire to the tip of the tube. This effectively creates a continuous actuatable joint at a much smaller scale than is possible with traditional joints. Nitinol is also already widely used in medical devices.

To select steerable sheath candidates to manufacture and test, we compared a selection of 16 sheath configurations simulation results. We tested sheaths with a steerable length between 5 and 20 millimeters, and a minimum bending radius between 3 and 18 millimeters. A visualisation for what these parameters mean can be found in Fig. 2.3.

All the steerable sheaths were simulated with 10 notches. With the manufacturing tolerances available, 10 is the maximum number of notches that we can use. Inner and outer tube diameters were dictated by the available stock material. The Nitinol tubing available had an inner diameter of 0.9 mm and an outer diameter of 1.1 mm. The depth of the notches was chosen to be 85% of the outer diameter based on empirical experience. This ratio only affects the mechanical strain on the spine and needs to be kept constant to test other curvature-dependent parameters, so varying notch depths were not tested.

Each set of parameters consisting of steerable length, radius, number of notches, tube inner and outer diameter are necessary and sufficient to calculate the notch height and spacing.

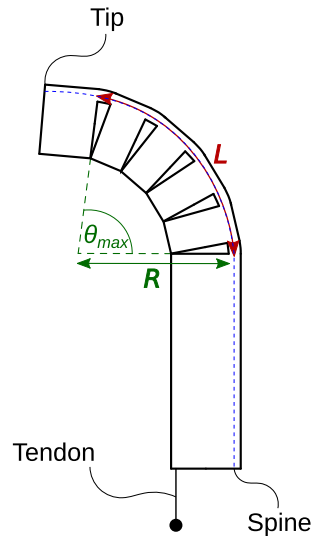


Figure 2.3: Visualisation of steerable sheath parameters. L is the steerable length. This is measured from the bottom of the lowermost notch to the top of the uppermost notch along the spine of the sheath. The spine is the neutral bending plane that runs through the uncut section of the sheath. It does not become stretched nor compressed. R is the minimum bending radius of the arc formed by the sheath when all notches are closed.

Each steerable sheath was modeled in MATLAB along with an endoscope sheath and a larynx model extracted from scans of cadaver larynges from Dr. Bailly’s group [14]. Not only does this visualization show us which steerable sheaths perform better than others, but that, in general, the data shows that augmenting the existing system with steerability significantly improves performance over the non-steerable baseline.

After the simulations were complete for all 16 steerable sheaths, the results were compared in a Table 2.1. This shows us general trends in how varying L and R values affect visible area. We chose a set of high performing steerable sheath configurations to manufacture and test with the rest of our system. After real world testing, we would pick a final steerable sheath design. Initially, four steerable sheaths were selected to be manufactured out of Nitinol. The four configurations are:

- $L=10$; $R=3$
- $L=15$; $R=8$
- $L=20$; $R=13$
- $L=20$; $R=8$

These configurations are represented as rows 5, 10, 15, and 14 respectively in Table 2.1. Each of these sheaths was chosen based on its high performance in simulation. We note that these simulation results not only provided us with data to chose which steerable sheath configurations

All Steerable Sheath Simulation Results

L (mm)	R (mm)	Visible Area (mm^2)
5	3	1720
5	8	1229
5	13	1089
5	18	977
10	3	2198
10	8	1916
10	13	1530
10	18	1285
15	3	2249
15	8	2212
15	13	1912
15	18	1758
20	3	2288
20	8	2264
20	13	2151
20	18	1947

Table 2.1: Summary of simulation results of all tested sheaths. L is steerable length and R is the minimum bending radius. The table shows the simulation result of each sheath configuration as the total visible area.

to manufacture, but they also support our initial claim that adding steerability to the laser fiber would greatly improve the viability of the procedure seen in Fig. 2.4.

2.3 Selection of the Laser Fiber

In-office treatment of laryngeal tumors hinges on the use of a laser fiber to deliver pulses to the tumor to eradicate it. The hollow lumen of the notched tube sheath allows the passage of the laser fiber along with a pull-wire tendon to bend the steerable sheath. As discussed in section 2.2, the steerable sheath geometry that enables visualization of the most area involves bending the sheath at very small radii. Therefore, we needed to determine:

- Whether the laser fiber is capable of bending in such small radii, and
- Whether the force required to bend the laser fiber and steerable sheath was less than 5N, so as to be easily actuated by the motors we planned to use.

Initial tests showed that the Endostat laser fiber (6-700 micron) currently used in-office prevents the notched tube from curving properly and bending completely. This causes concerns that the laser fiber might break if it is bent in the small radii achieved by our steerable sheaths. The thickness of these laser fibers also ultimately limits physicians' dexterity by preventing

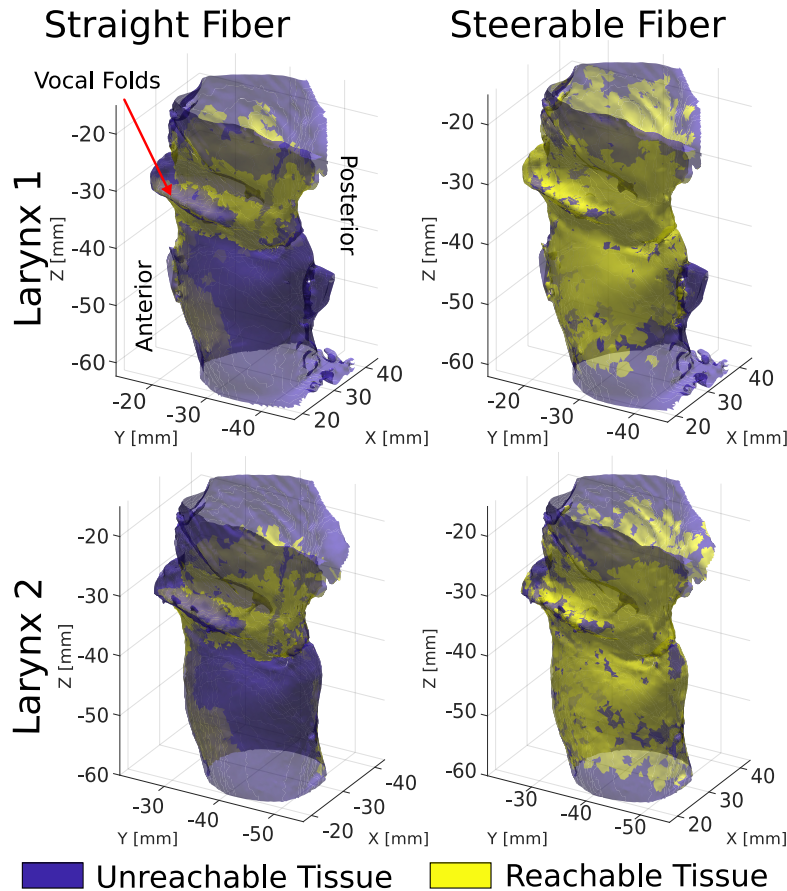


Figure 2.4: Comparison between steerable (right column) and non-steerable (left column) laser fiber. The top row is for the first larynx model and the second row is the second model. This comparison shows that the steerable laser fiber is able to reach significantly more tissue consistently across different larynges. The particular sheath configuration used to produce this result is $L = 10\text{mm}$; $R = 3\text{mm}$.

the steerable sheath from bending in the small radii it could in order to reach certain areas of the larynx. Therefore, thinner laser fibers (200 micron and 105 micron) were also considered as alternatives to the Endostat fiber.

The test setup shown in Fig. 2.5 was used to measure the force required to bend the sheath at 0.5 mm increment displacements of the pull-wire for each of the laser fibers and for several steerable sheaths of different geometries. The force sensor used is the IIT FT17 (Istituto Italiano di Tecnologia, Genoa, Italy), and the linear sliding stage is the Linear Slide – UniSlide A40 series with Graduated Knob (Velmex, Inc., Bloomfield, NY). The rotary stage is the A5990TS (Velmex, Inc., Bloomfield, NY). For each steerable sheath, the following cases were tested:

- **Case 1** – With an empty lumen.
- **Case 2** – With the 105 micron laser fiber.

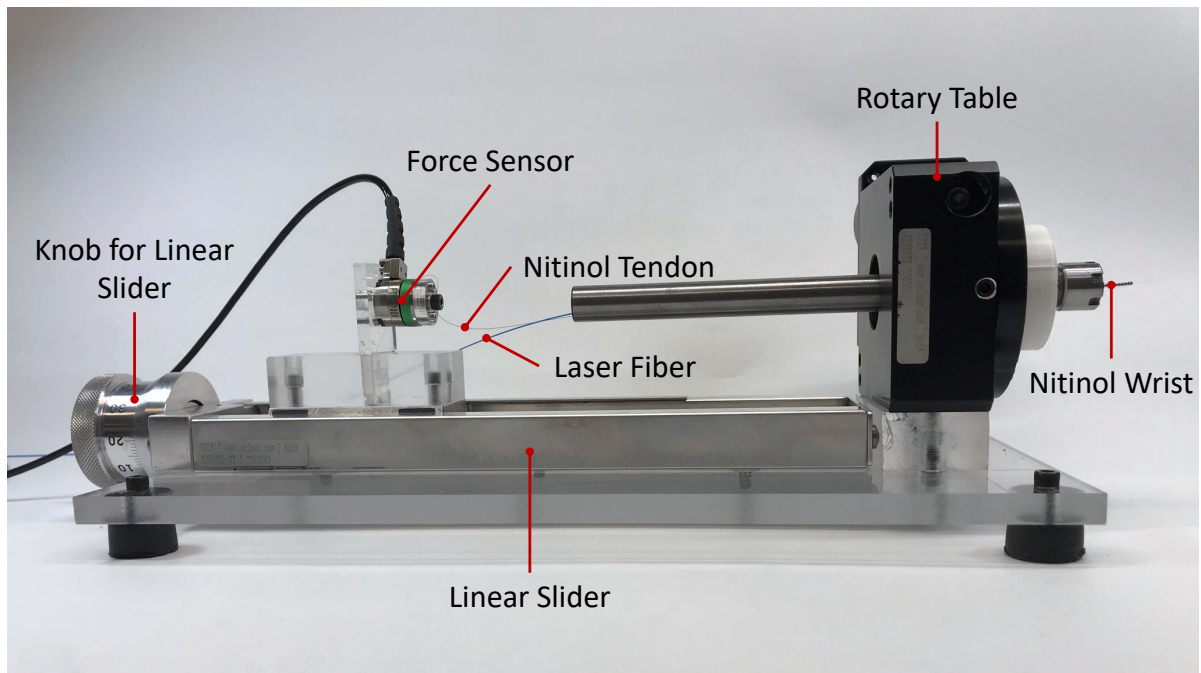


Figure 2.5: *Experimental setup used to test the force required to bend the Nitinol sheath with under 4 conditions: with an empty lumen, with a 105 micron laser fiber, with a 200 micron laser fiber, and with the Endostat laser fiber.*

- **Case 3** — With the 200 micron laser fiber.
- **Case 4** — With the Endostat laser fiber.

As shown in Fig. 2.6, these tests showed that the amount of force required to bend the steerable sheath with the 200 micron and 105 micron was comparable to bending an empty sheath, whereas bending the steerable sheath with the Endostat laser fiber required much more force. Thus, we decided to move forward with the 200 micron laser fiber. Another WPI team working with Professor Yuxiang Liu is working on a device to adapt the laser pulse machine's conventional Endostat laser fiber to the 200 micron laser fiber. Other factors that may need to be tested by a future team include investigating whether bending the laser fiber at such small radii results in significant power loss, and whether this power loss severely impacts the efficacy of laser pulse treatment.

2.4 Spring Coil

A hollow connector, or tube, is needed to connect the Nitinol sheath to the actuation unit. The spring coil must be hollow to enable passage of the laser fiber and tendon, and thin enough to fit through the endoscope's working channel. Furthermore, the spring coil must be flexible enough to follow the anatomical bends of the patient that will bend the endoscope working channel. Another

Tendon Displacement vs Pulling Force - 20 mm Steerable Sheath

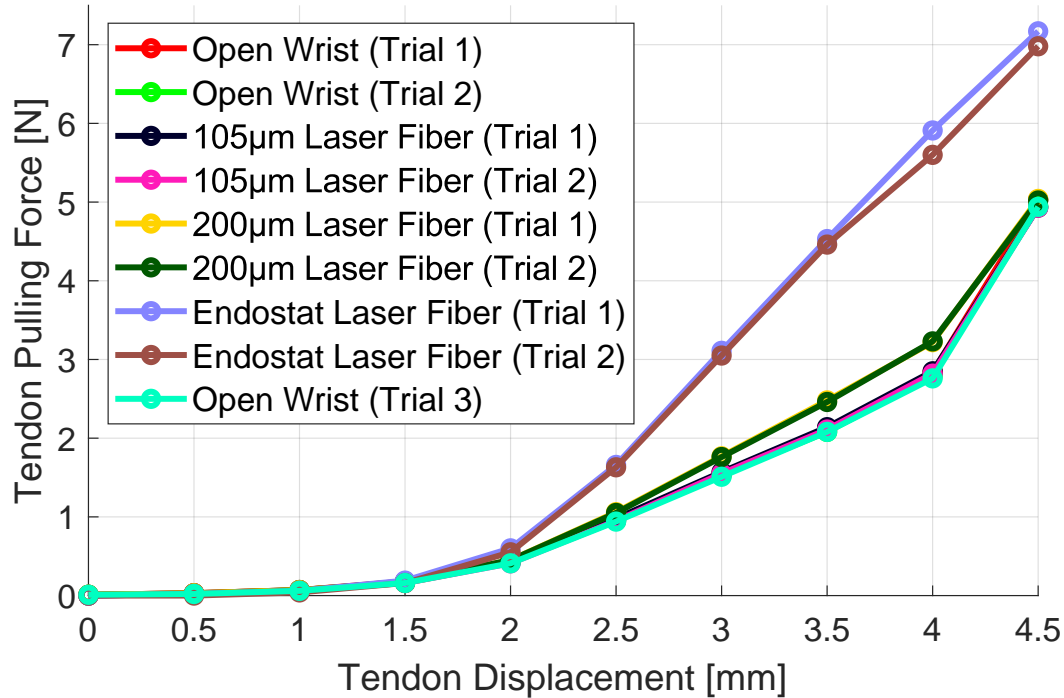


Figure 2.6: Graph showing amount of force exerted by the tendon, in N, as it is displaced to gradually bend the Nitinol sheath under different conditions: open sheath (no laser fiber), with a 105 micron laser fiber, with a 200 micron laser fiber, and with the conventionally used Endostat laser fiber. The Endostat laser fiber requires significantly more force to bend and does not allow the steerable sheath to close completely. Therefore, we elect to use the 200 micron laser fiber instead, which require comparably lower amounts of force to bend while inside the steerable sheath.

important consideration in the selection of the tubing is its ability to transmit rotational and translation within the endoscope working channel and while the endoscope's working channel is bent at an approximately 90 degree angle.

Our hypothesis was that two main factors determined how well a spring coil transmitted rotation in the endoscope working channel: thickness and friction. We posit that a higher diameter spring coil, specifically with thicker walls (high ratio of outer diameter vs inner diameter), transmits rotation better than a smaller one with thinner walls because of a larger polar moment of inertia. However, the friction between the operating channel and the spring coil also grows with the spring coil's diameter. This is because the spring coil would make more contact with the endoscope working channel as its diameter increases. The 2 mm diameter of the endoscope working channel limits the outer diameter of the spring coil. Once the spring coil's outer diameter is too large, friction overrides any benefits that come from a thicker spring coil. Therefore, we needed to find a spring coil that balanced these two considerations for optimal rotation transmission.

Several options were investigated, including plastic medical tubing, before metal alloy spring coils were selected as the most viable option. Experiments testing five spring coils were conducted. The objectives of the experiment were as follows:

- To measure how well different spring coils transmit rotation through the endoscope's working channel while the endoscope tip is bent at different angles.
- To select a spring coil that would best transmit rotation and translation through the working channel.

Fig. 2.7 shows the experimental setup. As part of the experimental setup, we manufactured several clear, angled acrylic caps that can be switched out to test different endoscope tip angles. These caps hold the tip of the endoscope's working channel at a certain angle to mimic how physicians usually are able to bend the tip of the endoscope working channel. We tested with the 0, 60, and 90 degree bends shown in Fig. 2.8. It is important to test the ratio of rotation that a spring coil tube is able to transmit at several different angles of the endoscope's tip because during surgery, physicians regularly bend the endoscope tip up to about 90 degrees, which increases the friction that the spring coil must contend with to properly transmit torsional forces. Therefore, we wanted to ensure that the spring coil tube we selected could still perform well under such circumstances.

For each experiment, the black rotary stage is hand-rotated so that the spring coil is moved in one full rotation (360 degrees). At the end of each experiment, the number of degrees travelled by the the other end of the spring coil at the white dial was recorded. For each spring coil, the experiment was repeated twice (clockwise and counterclockwise) for the following cases.

- **Case 1** – tip bent at 0 degrees
- **Case 2** – tip bent at 60 degrees
- **Case 3** – tip bent at 90 degrees

The results show that rotating the spring coil in one direction consistently performs better than in the other direction, supporting the hypothesis that spring coils rotate better if they rotate in the same direction that the coil is wound. Spring coils 1 and 3 showed particularly high rotation ratios and were thus selected for our device (Table 2.2). Spring coil 1 is 1.32 mm in outer diameter and 0.66 mm in inner diameter and is made of a rounded wire of 0.33 mm (The Dr. Templeman Co., Plainville, CT). Spring coil 3 is part of a biopsy forceps set from PENTAX. We tested the spring coil from PENTAX biopsy forceps model KW1806S with an outer diameter of 1.47 mm.

Based on these results, we selected for closer examination two spring coils that transmitted rotation the best: spring coils 1 and 3. Spring coil 3 seems to outperform spring coil 1 overall, having a higher average rotation ratio for both clockwise and counterclockwise rotation (Table

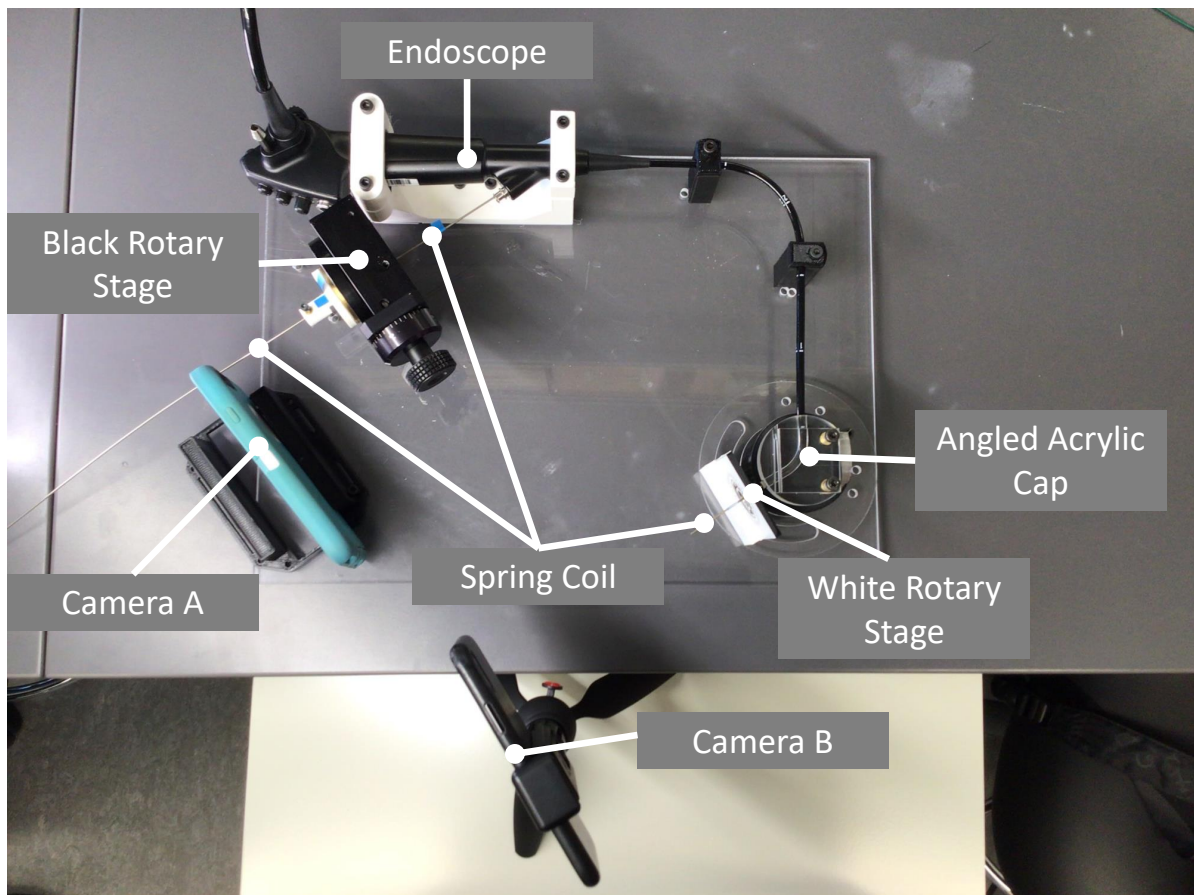


Figure 2.7: *Experimental setup for spring coil rotation tests to determine the ratio of rotation transmitted by 5 spring coil candidates.*

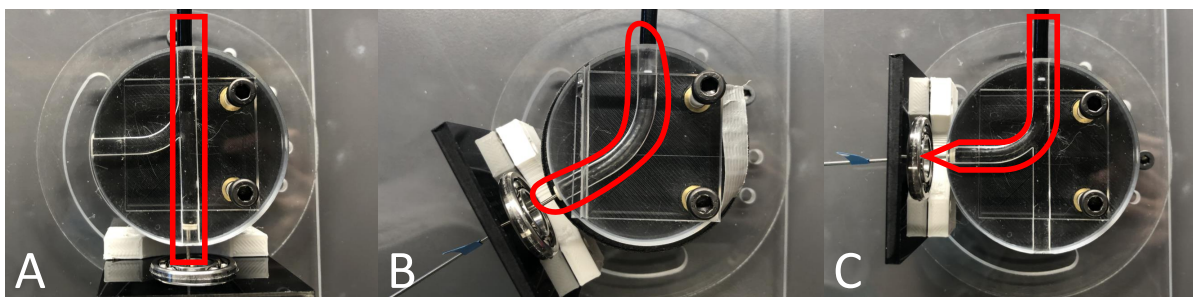


Figure 2.8: *Three tip angles used for testing spring coil candidates for ratio of rotation transmitted in both directions (CW and CCW): A) 0, B) 60, and C) 90 degrees.*

Spring Coil Number	Product Name	CW Ratio	CCW Ratio
1	SG-052-013-44	0.97	0.42
2	OLYMPUS FB-211D	0.61	0.51
3	PENTAX KW1806S	0.92	0.53
4	ConMed 100507	0.81	0.56
5	SG5-052-010-016-120	0.18	0.07

Table 2.2: Ratio of rotation transmitted in each direction of rotation, under Case 1: tip bent at 0 degrees.

2.2). However, spring coil 3, taken from the PENTAX KW1806S forceps, were \$400 each (only 110 cm of spring coil can be obtained from each pair of forceps) [15]. On the other hand, Coil 1, SG-052-013-44 spring coil, is much more affordable (\$6.20 for 110 cm of spring coil) [16]. Therefore, the spring coil used in our device is the SG-052-013-44 spring coil.

2.5 End Effector Cap

In order to accurately steer the laser fiber, the laser fiber must properly follow the curvature of the steerable sheath. This ensures that the fiber stays in line with the center line of the steerable sheath and is aimed where the controller intends. Without an end cap, this does not happen (Fig. 2.9). Furthermore, the tendon for actuating the steerable sheath needs to be attached to the steerable sheath. The existing procedure was to glue the tendon to the outermost notch of the steerable sheath, but this takes much time and skill, and often results in mishaps where glue gets into the notches and prevents them from closing properly. Therefore, the end cap needed to have holes for both the laser fiber and holes for tying the tendon. A similar solution was found in the literature [13]. The main challenge in finding a suitable end cap was the steerable sheath's extremely small size. This necessitated the design and construction of a custom end cap (Figure 2.10). The end cap used in the final design is made by laser cutting layers of the cap out of stainless steel sheets and stacking them with glue to form the end cap shape. The final dimensions of the end cap are as follows: the diameter of the top surface is 1.1 mm and the diameter of the bottom section is 0.85 mm. The end cap is 0.6 mm thick in total.

2.6 Actuation Unit

The actuation unit is the component of the device which encompasses the motors and gears needed to manipulate the steerable sheath at the end of the endoscope. This unit needs to be able to translate the steerable sheath linearly, rotate the steerable sheath, and flex the steerable sheath. The design goal of the actuation unit is to have a highly compact device that has these three degrees of freedom. We decided that the best location for the actuation unit would be

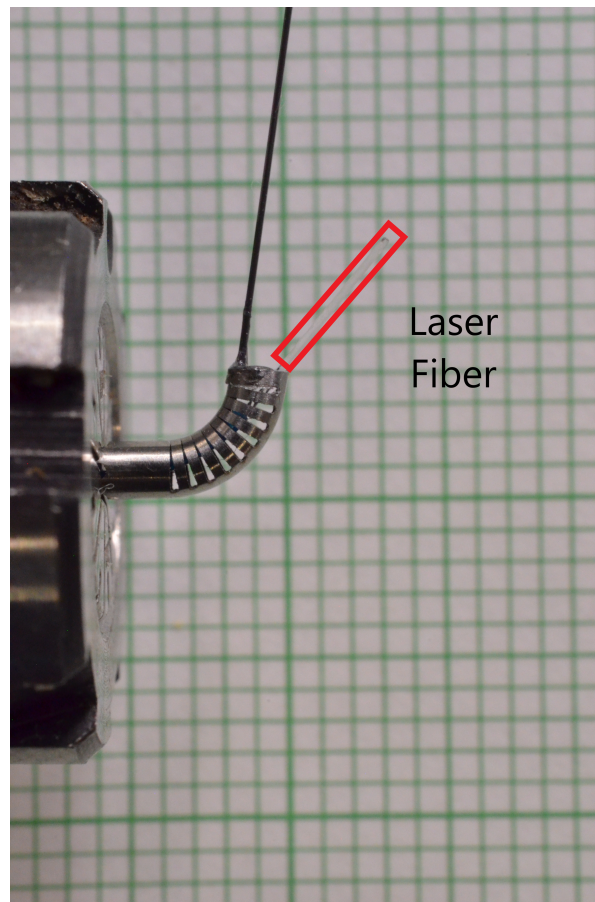


Figure 2.9: *Steerable sheath shown fully bent with laser fiber tangentially following the outer arc of the steerable sheath's curvature, not aligned with the centerline of the steerable sheath, which the Nitinol tendon is parallel to.*

directly mounted onto the endoscope, which would limit the amount of cable in a physician's way while using this device.

An early design used a linear slider to provide translation of the laser fiber, however it soon became apparent that this solution would have made the integration of our device in the clinical workflow difficult. The linear slider is relatively bulky, and it would have added considerable weight to the device, which has to be hand-held by the operating physician. We therefore explored an alternative solution to provide translation. Taking inspiration from a design recently published in the biomedical literature [7], we created a new design where the optical fiber is threaded through a hollow lead screw (Translation Leadscrew in Fig. 2.11). This solution enables a drastic decrease in the size of the actuation unit, while still enabling translation of the laser fiber. The final design is a 2.5 cm diameter cylinder with a 10cm height and weighs only about 100 g total, 130 g with the motors included. An overview of the final device is shown in Fig. 2.11.

The lead screw is attached to the spring coil and translated linearly through the rotation of the lead screw nut. The linear action of the actuation unit can be driven by a motor that is

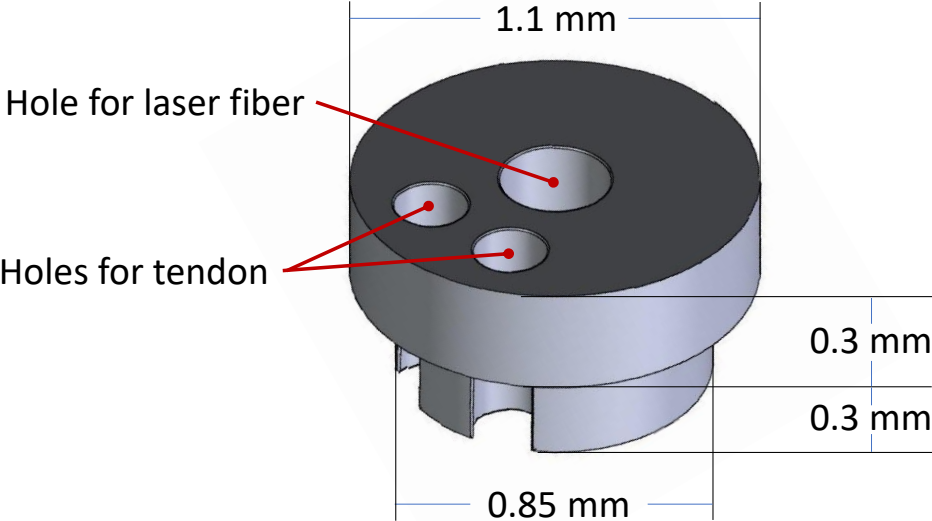


Figure 2.10: End cap design. Two holes are for the Nitinol tendon to be attached through, and the hole in the center is for centering the laser fiber in the steerable sheath so that it follows the centerline of the bending steerable sheath’s curvature.

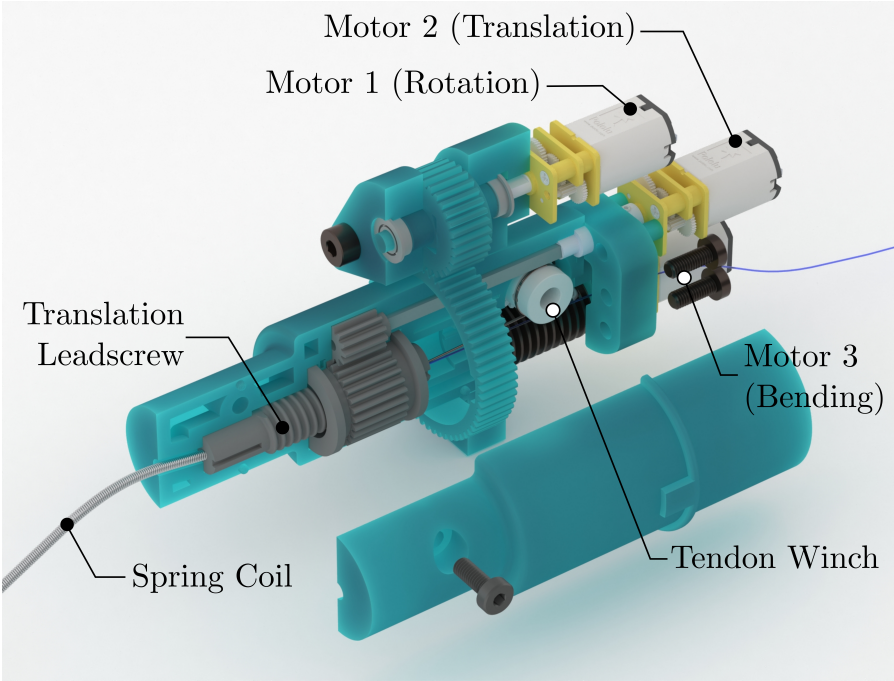


Figure 2.11: Exploded render of actuation unit showing main components.

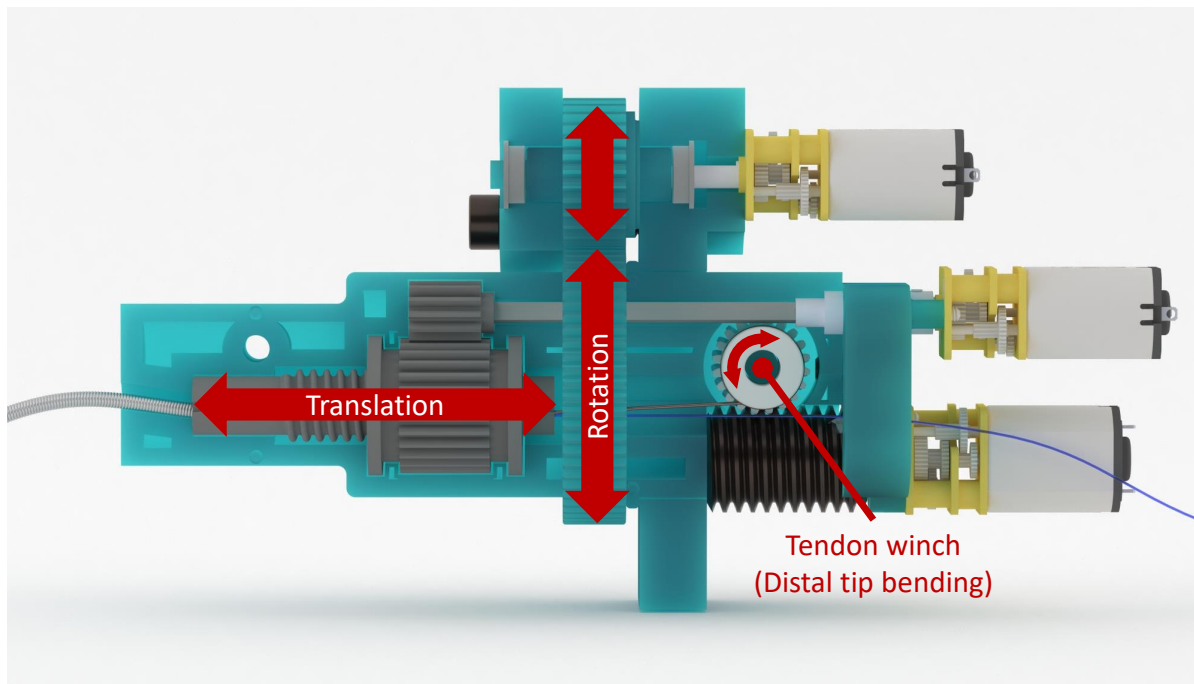


Figure 2.12: Side view of the actuation unit opened to show internal components. The lead screw enables translation of the laser fiber, two gears on the outside of the actuation unit enable rotation, and a tendon winch enables bending of the steerable sheath and laser fiber.

placed on the rear of the actuation unit using a connection shaft. To flex the steerable sheath, the tendon is attached to both the steerable sheath and a winch, which is actuated by a worm gear. The rotation of the winch pulls and releases the tendon depending on the direction of rotation, flexing the steerable sheath. Lastly, a gear encases the outside of the housing and meshes with a smaller gear attached to a motor. This allows the gear to rotate the entire actuation unit, thereby rotating the laser fiber. These three degrees of freedom are summarized in Fig. 2.12.

The laser fiber and spring coil is attached to the hollow lead screw using adhesives, so that the laser fiber can translate linearly and rotate along with the lead screw. The tendon is passed through the hollow center of the lead screw and attached to the tendon winch. The design has the advantage of being small and lightweight. However, the linear translation of the hollow lead screw bends the steerable sheath, because the tendon is fixed to a winch located behind the lead screw, which does not advance as the lead screw does.

The motors used in the actuation unit are Polulu 6V high powered motors (Micro Metal Gearmotor HP 6V, Polulu Corporation, Las Vegas, NV), which are needed for their high extrapolated stall torque compared to the 6V low powered motors or high powered carbon brushed equivalents [17]. Testing with 6V low powered motors showed that these motors were not able to overcome the friction present in the system to properly translate or rotate the laser fiber. Based on preliminary controllability and speed calculations, two gear ratios were selected: 1:298 for rotation and 1:380 for translation and tendon bending (see Section 3.2 for these calculations).



Figure 2.13: Existing office-based laser surgery setup. Both of the physician’s hands are occupied. Reproduced from [8].

2.7 Controller

In the current office-based procedure, both the physician’s hands are occupied (see Fig. 2.13). If the physician is right-handed, their right hand holds the endoscope handle. Their right thumb controls the distal bending of the endoscope tip, leaving severely limited mobility for the other fingers on the right hand to operate other buttons and controls. The physician’s left hand holds the endoscope and the patient’s face, serving to prevent the endoscope from coming out of the patient’s nose and to anchor the physician to the patient. Since the physician is looking at the computer screen showing a live video feed from the endoscope’s chip-tip camera and not the patient, placing their left hand on the patient enables them to use proprioception to maintain the proper posture in relation to the moving patient.

To control the actuation unit, our team envisioned a clip-on device to the endoscope that would enable the physician to control both the endoscope and steerable laser with their right hand. This solution would also enable us to simplify our device and minimize complexity by combining the actuation unit and its controller. To make the on-handle actuation unit and controller a feasible solution, the device needs to be:

- Lightweight (at least as light as the existing endoscope handle) so as minimize the physician’s discomfort, and
- Ergonomically placed to make control of the actuation unit possible and comfortable with the right hand.

The control panel is made up of six buttons, an ESP32 microcontroller (Espressif Systems, Shanghai, China), and two L293D dual H-Bridges (Adafruit Industries, New York, New York).

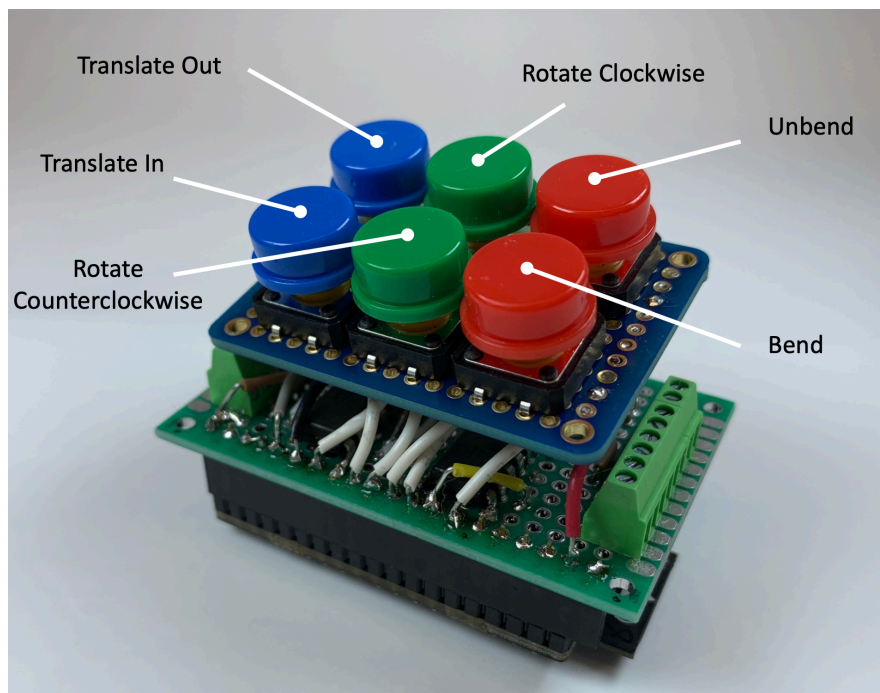


Figure 2.14: Custom-made button panel to control three degrees of freedom using the actuation unit to control the laser fiber. Designed to be mounted in a box directly onto the endoscope, enabling one-handed control of the actuation unit.

The buttons are separated in to 3 pairs with each pair controlling a degree of freedom for the steerable sheath, either translation, rotation, or bending (Fig. 2.14). When each button is pressed, its output is switched from ground to 3V. The outputs of the buttons are connected to input pins on the ESP32. To precisely control the device, we decided to use the ESP32 to handle the user inputs from the buttons and control the correct motors. The wiring diagram for this custom-built control panel is shown in Appendix B.

The main reason the ESP32 is needed for motor control is that translating the laser fiber affects the bending of the laser fiber. For example, when the laser fiber is translated out of the endoscope, the steerable sheath bends slightly because the tendon fixed at the laser fiber tip is connected to the tendon winch in the actuation unit, which is not translated. To decouple these degrees of freedom, the ESP32 controls both the bending and translation motors when translating the steerable sheath. For the ESP32 to control a motor, the L293D H-bridge is used because the ESP32 cannot supply the 6V the motors require. The H-Bridges act like a series of electric switches that can send power to the motor, switch the directions and stop the motor based on the inputs from the ESP32. Furthermore, each H-Bridge has an enable pin that can be pulsed with a Pulse Width Modulation signal that can rapidly turn the H-Bridge and motor on and off in order to control the motor speed. Each L293D can control two motors bidirectionally. Each motor has encoders which are also connected to the ESP32 so our microcontroller can keep

track of the position of each motor for actuation unit control.

With each motor's rotation tracked, we set boundary limits for each of the encoder values preventing the actuation unit from damaging itself by rotating a motor too far in one direction. Using both the encoder values and the variable speed, the motors are able to be controlled using PID to precisely control the rate of translation motor speed and the bending motor speed during translation. Lastly, a small screw terminal block is used to connect the external power source that connects to the H-Bridges, and eventually the motors, providing the 6V that the motors require to operate at maximum efficiency.

INTEGRATION AND TESTING

In this section, we report on the testing and validation of our design. First, we evaluated whether the design successfully fulfilled the mechanical constraints and requirements of the project. During these tests, we also executed reliability testing to determine the effect of wear and tear on the device.

3.1 Integration

The design includes several tiny parts that need to fit together precisely, especially within the actuation unit itself. Most of the parts are 3D printed and can easily be assembled together. The fully integrated device is shown in Fig. 3.2. The device is broken down by a few main sections: the steerable sheath assembly, the actuation unit, and the control panel.

Steerable Sheath Assembly The components of the steerable sheath assembly include one of each of the following: a Nitinol notched tube, a length of spring coil tubing, an end cap, a Nitinol tendon, and a laser fiber. First, the Nitinol tendon is looped through the end cap and glued to the inside. Then, the end cap is placed at one end of the Nitinol steerable sheath. The laser fiber can be passed through later. This end cap is also glued to the Nitinol steerable sheath. The spring coil tubing is then attached to the Nitinol steerable sheath using heat shrink medical-grade tubing. The spring coil will be glued to the translation leadscrew, and the Nitinol tendon is fixed to and wound around the tendon winch. This assembly is rendered in Fig. 3.1.

Actuation Unit First, the internal components of the actuation unit need to be assembled. The leadscrew and tendon winch are placed into their locations in the housing, taking care to align the slats on the leadscrew with the corresponding location on the housing. The tendon

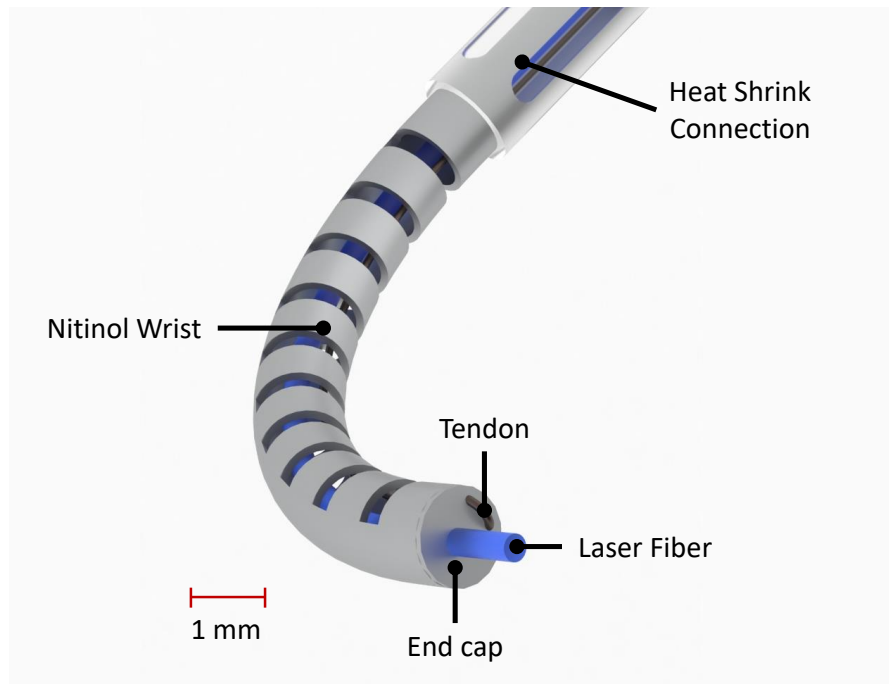


Figure 3.1: End cap design integrated with Nitinol steerable sheath, laser fiber, and tendon.

winch is inserted into its hole and the small gear and shaft above the translation leadscrew are also inserted. Finally, the housing can be closed and screwed shut with a single screw. The large rotation gear is fitted on the closed housing. Motors can be aligned with their shafts after the actuation unit is closed. Using our custom-made mounting apparatus, the housing unit is aligned with the working channel of the endoscope. The mounting unit also has a place for the smaller rotation gear assembly which is attached to the rotation motor.

Control Panel The wires for the motor and for power should first be attached to the proper screw terminals on the electrical board. Then, the electrical board can be inserted into the custom-made box holder with the ESP32 port facing the opening in the back of the box. Finally, the front plate is screwed on top of the buttons. The box that houses the control panel has its own mounting unit and is firmly attached to the backside of the endoscope.

3.2 Mechanical Design Evaluation

Once all of these components were integrated with the endoscope, we were able to verify that we could control the laser fiber in three degrees of freedom to the extent that we set as our goal at the beginning of the project. At first, there were significant issues with friction due to the quality of the 3D print in the actuation unit, and the motors we purchased did not have enough torque to overcome these friction issues. Because the actuation unit is so compact, there were

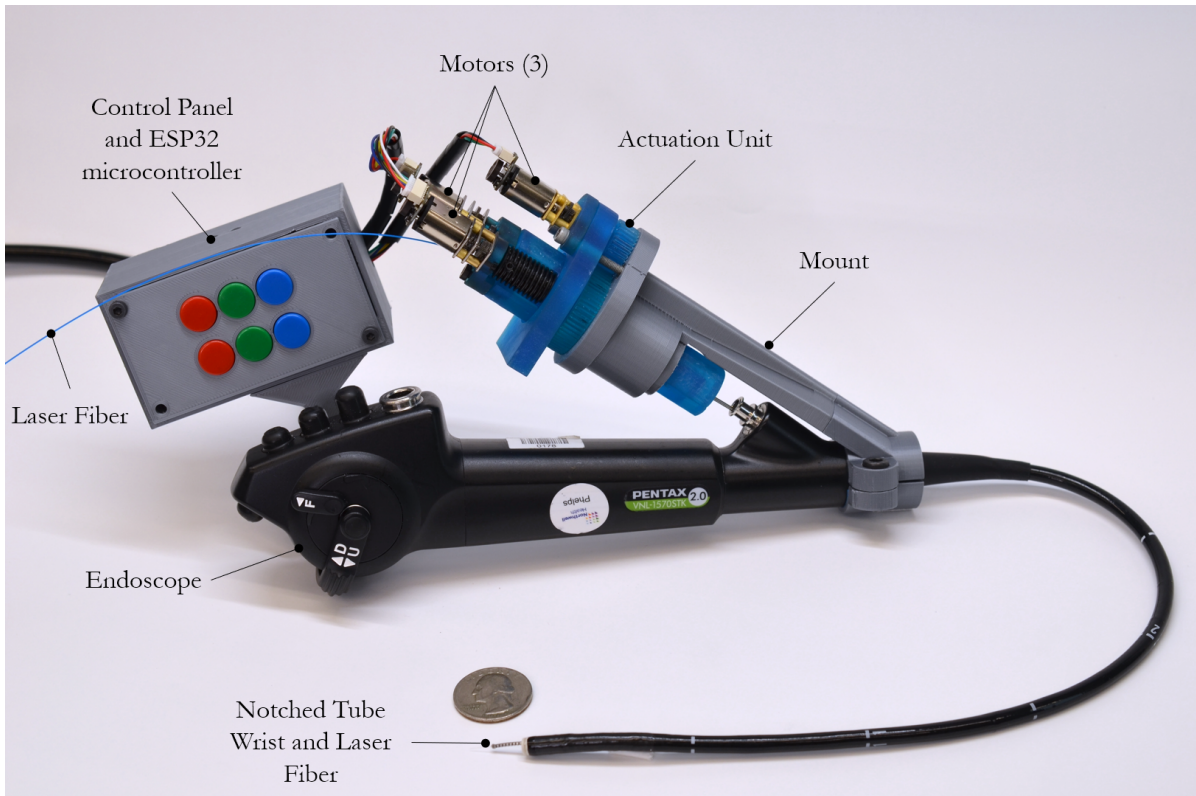


Figure 3.2: Fully integrated device, showing the button panel and actuation unit mounted on top of an endoscope that is currently used in office-based laser surgery of laryngeal tumors.

very tiny tolerances which gave rise to these issues. However, once we performed post-processing, i.e., sanding down certain parts and replaced standard motors with high-powered ones, we were able to easily actuate all three degrees of freedom.

To test each degree of freedom, we used the custom-made testing jig that was also used to test the spring coils (see Section 2.4); more specifically, the jig was used to hold the endoscope in a bent configuration that approximates the anatomical bend of the nose and throat. The test setup is shown in Fig. 3.3. The control panel is unmounted from the endoscope because it would be face-down if kept on the endoscope due to the orientation the endoscope must be in to fit into the testing jig. A detail of the test setup, where the camera is placed above the tip of the endoscope, is shown in Fig. 3.4. When testing translation, an acrylic cap used in spring coil testing was used to hold the endoscope tip in place (see Section 2.4).

3.2.1 Steerable Sheath Bending

Out of the four geometries manufactured for this project, the steerable sheath used in testing was 10 mm long with a 3 mm bending radius. To test how far the steerable sheath can bend the laser fiber, we took pictures while the steerable sheath was fully bent and fully straight,

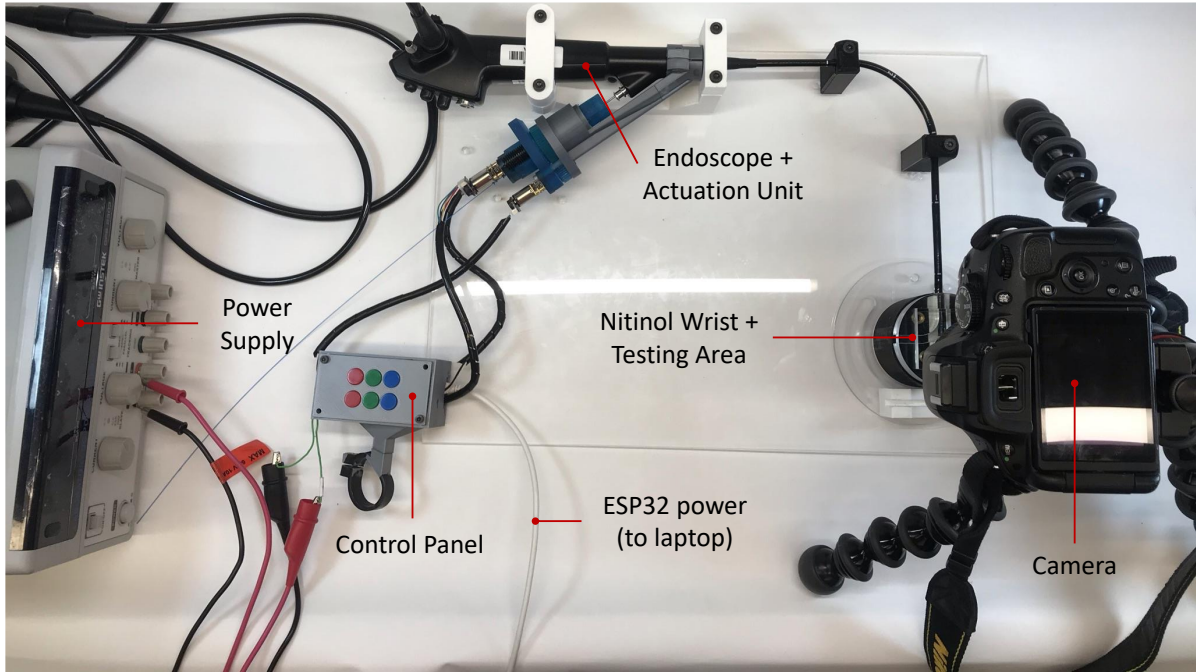


Figure 3.3: Test setup used for verification testing of the device.

then used an online protractor to measure the angle between these two position [10]. Though the steerable sheath was designed to be able to bend almost 190 degrees, we did not attempt to achieve such an extreme bending angle because of concerns that the tendon would detach itself from the end cap at the tip of the steerable sheath. Because we only have 3 end caps to test, we did not want to risk damaging one. As seen in Fig. 3.6, the steerable sheath could be bent 80 degrees. The progression of the bending of the steerable sheath is shown in Fig. 3.5. We observed some unusual bending behavior where the notches closer to the base of the steerable sheath seem to close but the notches along the rest of the steerable sheath do not. Even if we continued to press the button for the tendon winch, we did not witness any additional bending of the steerable sheath past about 80-90 degrees. The cause of this additional stiffness should not be the laser fiber, since we already verified that using the 200 micron laser fiber in the steerable sheath does not interfere with its bending (see Section 2.3). However, during previous testing, the steerable sheath did not have as small of a bending radius as the current geometry. The effect of this factor could be investigated in the future.

According to our calculations, the steerable sheath should take about 2.92 seconds to go from fully straight to fully bent. Full bending requires a tendon displacement of about 4.5 mm, and the actuation unit can theoretically wind up the tendon at 1.54 mm/s (Equation 3.1).

$$(3.1) \quad 1.4 \text{ motor rps} \times \frac{1 \text{ pinion gear rotation}}{20 \text{ knob rotations/worm rotation}} \times \frac{7 \times \pi \text{ mm tendon displacement}}{1 \text{ pinion gear rotation}} = 1.54 \text{ mm/s}$$

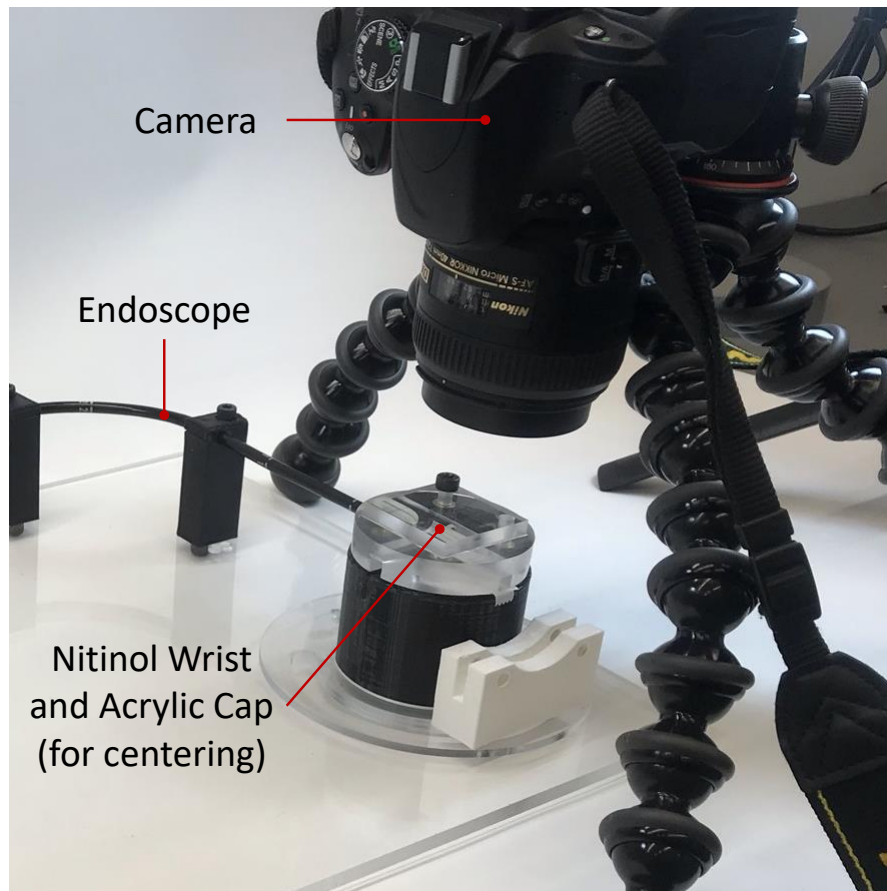


Figure 3.4: Camera and testing area setup for verification testing.

During testing, it took an average of 3.33 seconds to fully bend the steerable sheath. This results in a 13.9% error between our theoretical and experimental calculations. The actual speed is less than the theoretical speed, which is expected because the motor rotation speed used in our theoretical calculations is the no-load speed. In the actual device, there is considerable friction that is not negligible and likely explains this discrepancy.

3.2.2 Translation

We were able to translate the tip of the laser fiber by 14 mm, more than the full length of the steerable sheath. To determine this value, the endoscope tip was straightened and engineering paper was placed underneath the steerable sheath. Using the control panel, the distance the steerable sheath could translate in and out of the endoscope was measured. It should be noted that depending on how long the spring coil is cut to be, the starting position for the steerable sheath could be completely inside the endoscope working channel, and therefore the translation distance that can externally be observed could be less than the total displacement enabled by the lead screw. Theoretically, the lead screw allows for 16 mm of translation. The total translation we

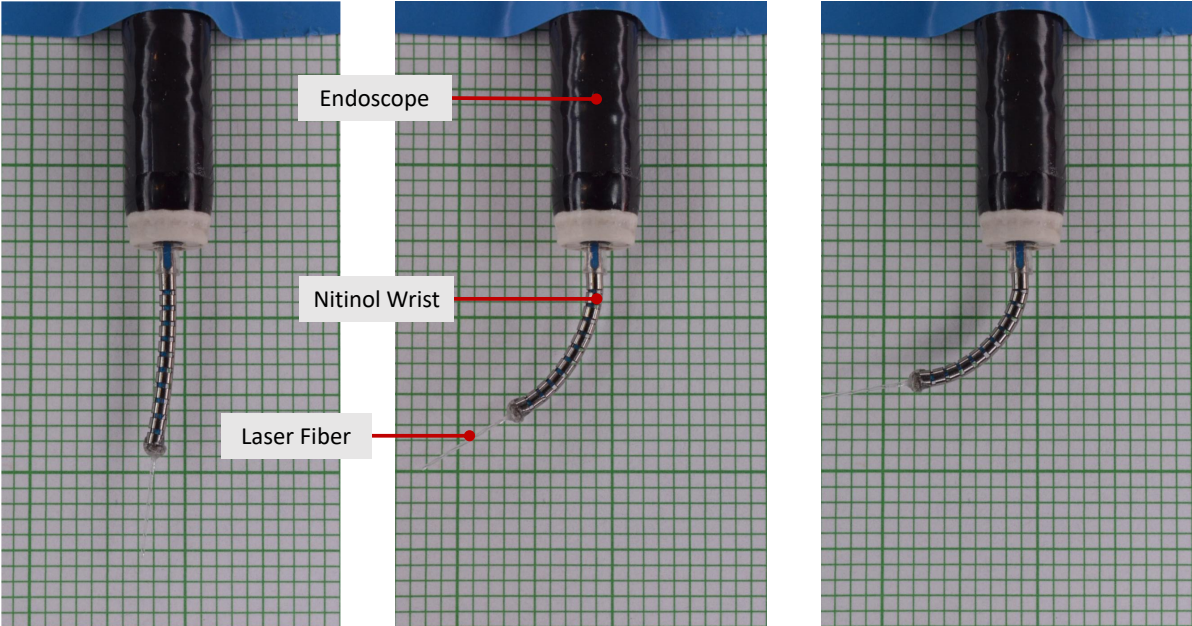


Figure 3.5: Stages of bending the steerable sheath from straight to fully bent, with the laser fiber inside the steerable sheath.

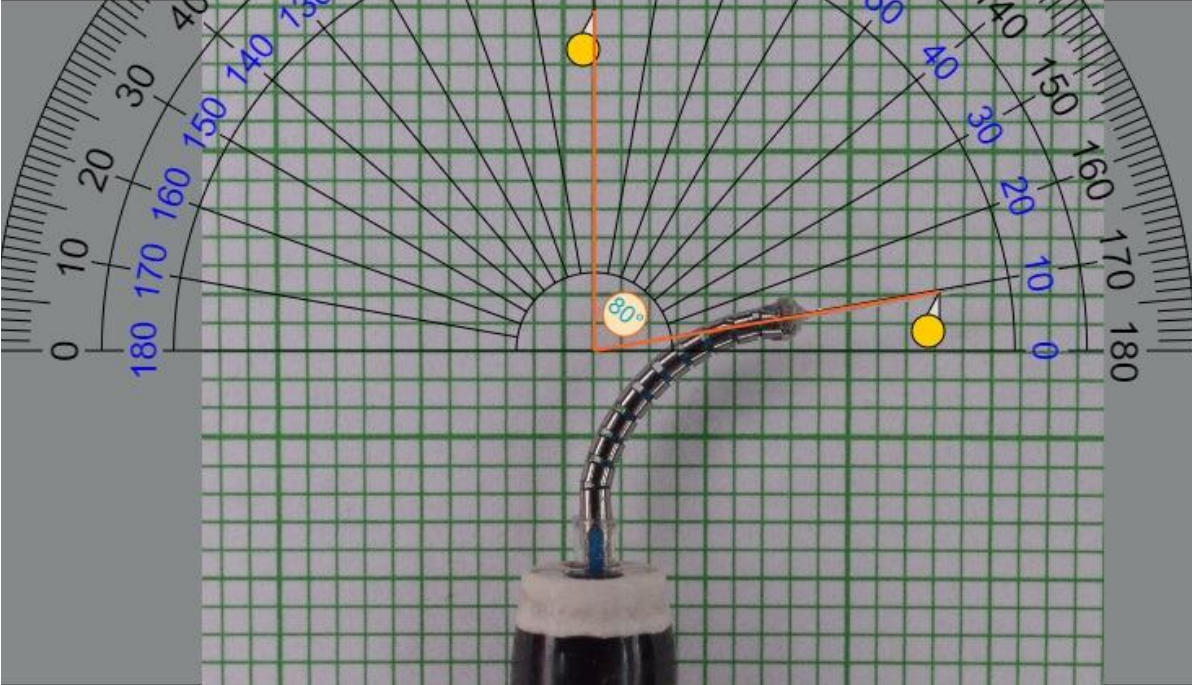


Figure 3.6: Full bending of the steerable sheath to 80 degrees. Created using online protractor tool [10].

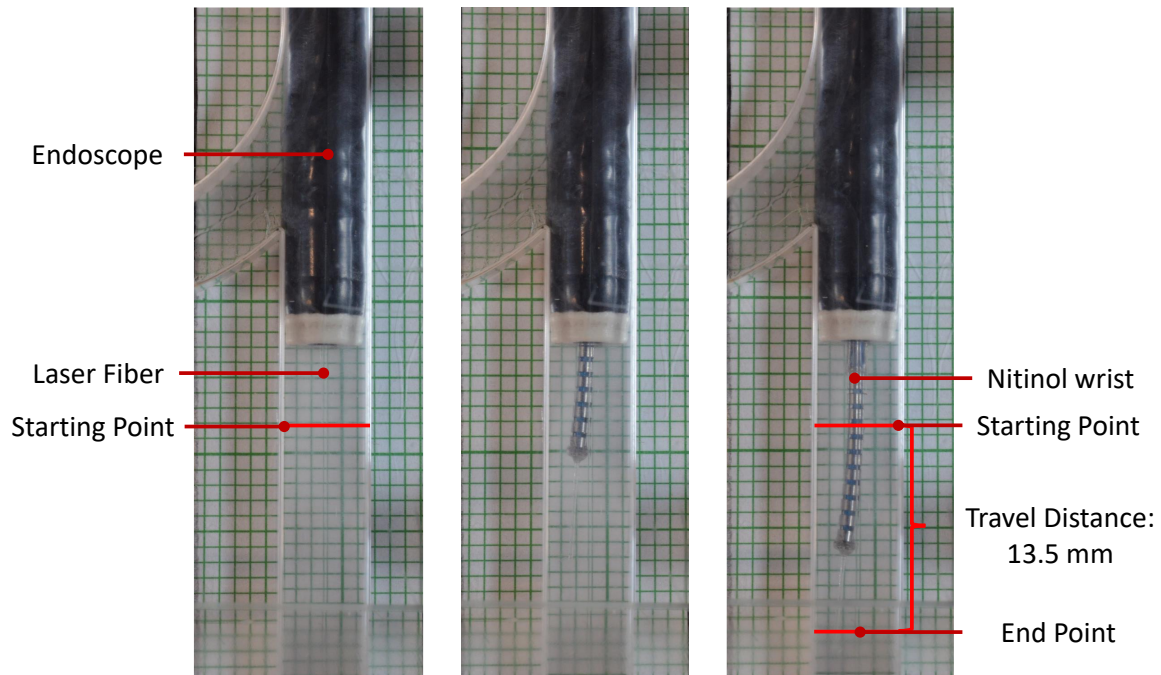


Figure 3.7: Stages of full translation using the device. In this trial, the device translates the steerable sheath 13.5 mm. The starting and end points are measured from the tip of the laser fiber since the tip of the steerable sheath is not initially visible.

observed was about 14 mm (average value over 3 trials).

According to our theoretical calculations, each rotation of the motor results in 0.643 mm of translation (Equation 3.2). This number is multiplied with the no-load speed of the motor, which is 1.4 rotations per second (rps). This results in an extension speed of 0.9 mm/s. Multiplied by the total distance that is able to be translated (1.6mm) results in a total extension speed of 17.8 s to fully translate the steerable sheath.

$$(3.2) \quad 1 \text{ motor rotation} \times \frac{12 \text{ lead nut rotations}}{28 \text{ motor rotations}} \times \frac{1.5 \text{ mm travel}}{1 \text{ lead nut rotation}} = 0.643 \text{ mm/motor rotation}$$

During testing, it took an average of 23.8 seconds to fully translate the steerable sheath. This results in a 33.8% error between our theoretical and experimental calculations. The slower actual speed compared to the theoretical value is expected because the motor rotation speed used in our theoretical calculations is the no-load speed. In the actual device, especially for translation, there is considerable friction, which likely explains this discrepancy.

3.2.3 Rotation

We were able to rotate the actuation unit more than 360 degrees—rotation is really only limited by the wires from the two motors in the middle twisting to a dangerous degree. During testing, we also observed the effect that we had seen when selecting a spring coil: rotation is consistent

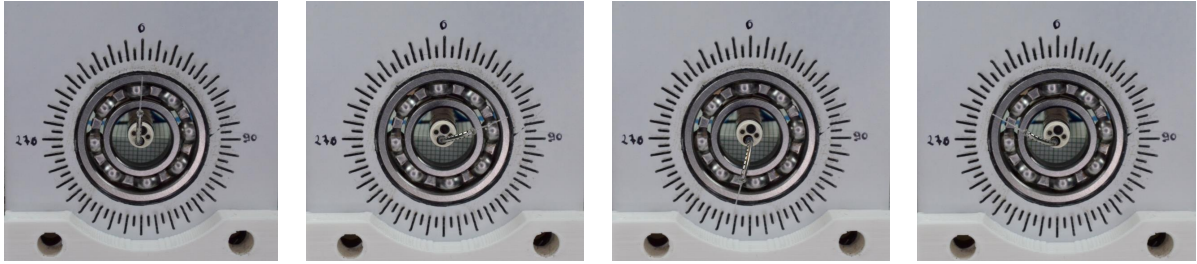


Figure 3.8: Sequence of full rotations using the device. The laser fiber and steerable sheath are at their fully bent position so that the laser fiber can be used to mark the rotation of the steerable sheath.

and controllable in one direction, but rotating in the other direction in the opposite direction that the spring coil is wound results in decreased controllability and snapping. When rotating in the opposite direction of the coil, pressing the button to move the rotation motor does not consistently result in rotation of the steerable sheath. However, rotation is very consistent when rotating in the direction of the coil, and we are able to easily rotate the device 360 degrees, as seen in Fig. 3.8.

According to our calculations, the actuation unit should be able to rotate the housing at 0.833 rotations per second. This means that it takes 1.2 seconds to rotate the housing once (Equation 3.3).

$$(3.3) \quad \frac{1.67 \text{ motor rotation}}{\text{s}} \times \frac{30 \text{ outer gear rotations}}{60 \text{ motor rotations}} = 0.833 \text{ rot/s}$$

During testing, it took an average of 2.06 seconds for each rotation of the steerable sheath. This results in a 71.8% error between our theoretical and experimental calculations. Again, the slower actual speed is expected because of the load due to friction in the system.

3.3 ENT User Study

During the project, we developed an experimental protocol that can be used to field-test our device with laryngologists or ear, nose, and throat (ENT) doctors who regularly performed office-based laser surgery for removing laryngeal tumors. This experiment can be used by the next SCREAM team or by students working on this project this summer to assess and iterate on our current design based on feedback. The experimental protocol is located in Appendix C.

DISCUSSION AND FUTURE WORK

4.1 Advancement Over SCREAM 2.0

In this project, we hoped to raise the TRL of this device from TRL 3 (Proof of Concept) to TRL 6 (Prototype). The Technology Readiness Level (TRL) scale was developed by NASA to rate the progress of a device from idea to fully working product ready for deployment [18]. The previous project team, SCREAM 2.0, created a device that was at TRL 3, the Proof of Concept stage. Their device illustrated the possibility of using concentric agonist-antagonist robotic (CAAR) manipulators, and demonstrated a feasible method of controlling this manipulator in the same three degrees of freedom as we hope to be able to control [9]. However, their device was not ready to be deployed in the office-based laser surgery setting, as it was not at scale. At the outset of our project, we set our goal for TRL 6, where a prototype of the device is constructed and ready to be tested in a similar environment to the target one. We achieved this goal, since our device is ready to be used for field tests by laryngologists in cadavers or ex vivo porcine larynges. During our project, we also designed an experimental protocol for these experiments (see Appendix C).

A comparison of the three project teams thus far is shown in Fig. 4.1. SCREAM 1.0 proved that a Nitinol continuum steerable sheath could be controlled in three degrees of freedom (rotation, translation, and distal tip bending) [6]. SCREAM 2.0 investigated a robotic platform for the automation of this control in a model that was not at-scale, and examined the use of CAAR tube manipulators [9]. Our device greatly simplifies the actuation unit design and integrates fully with the endoscope in an at-scale prototype.

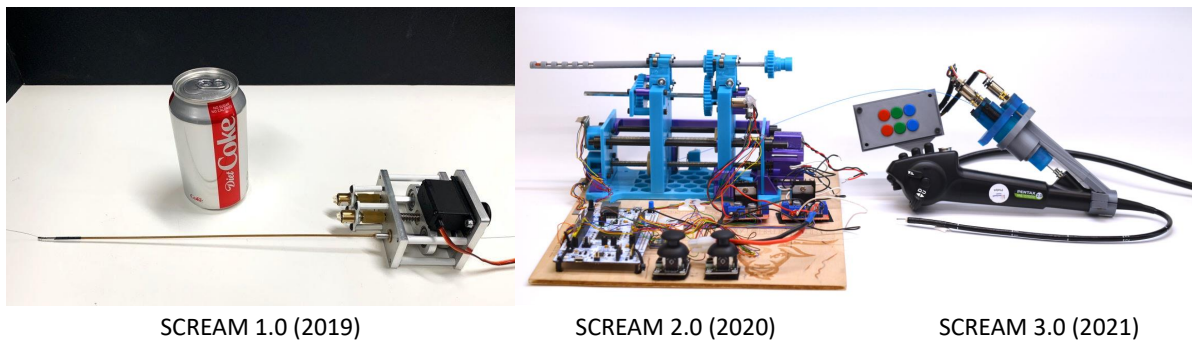


Figure 4.1: *Progression of design across the past 3 years of SCREAM.*

4.2 Future Work

4.2.1 User Study

Next year’s SCREAM team and students working over this summer will use our device and our experimental procedures to assess the efficacy and ergonomics of our device with laryngologists. We present a tentative experimental protocol in C. A preliminary application for approval from WPI’s Institutional Review Board (IRB) has already been submitted. Next year’s participants would need to finalize the experimental protocol and also apply for approval from the IRB at Brigham and Women’s Hospital, since the experiments will take place there. A structure to hold the ex vivo porcine larynx to be used in these studies also needs to be designed and manufactured. Based on the feedback from participants, it is likely that another iteration of this device will be designed, constructed, and evaluated.

4.2.2 Actuation Unit

We believe that the actuation unit’s current design provides an excellent solution for providing three degrees of freedom in the most compact and lightweight package. A possible avenue of inquiry will be into using at-scale CAAR tube manipulators to simplify the actuation unit design. CAAR tube manipulators would solve multiple issues currently present in our design. As discussed, rotation is consistent only in one direction (in the direction the spring coil is wound). A CAAR tube manipulator would decrease the need for much rotation, since the physician would be able to bend the laser fiber back and forth. Furthermore, the Nitinol tendon used in our device often unwinds itself from the winch and there is currently no way to prevent it from doing so. Although it still functions properly and is able to bend the steerable sheath, this causes changes in the controllability speed since the tendon is not being wound around the winch as intended but about the base of the winch, which has a smaller diameter than the winch itself.

4.2.3 Controller

Based on the current placement of the control panel, we posit that the buttons could be more easily accessed by physicians if they were moved closer to the actuation unit. The fix for this would be to modify the current 3D printed design for mounting the control panel box onto the endoscope. User studies may also reveal that physicians prefer the button panel to be in a different orientation than the current design for intuitiveness of use. It will be important to make sure that the device will smoothly integrate into the existing surgical workflow, particularly with supplying power to the system. Currently we supply power to the controller and motors with a bench-top power supply, which could not be used in an in-office surgery setting.

Due to the compact and difficult to manufacture control system, we also encountered multiple instances during validation testing of soldering coming undone inside the control panel, as well as spotty electrical connections. A custom-made PCB board would greatly improve how easy it is to troubleshoot the device when motors stop responding to button presses, for example. A PCB could also reduce the form factor of the control panel box. We also believe that the control panel box should be modified to allow for easier switching or maintenance of the motor wires and ESP32. The current design has fewer holes and easy-access slots than is ideal. Again, this would require a modification to the current 3D printed design.

To finish coupling the motion between translation and bending, the PID controller needs to be implemented in the motor control code. With the PID implemented, the bending will be able to be precisely controlled relative to the translation in order to prevent the coupling problem between translation and bending causing sheath bending. However, getting the control to be precise will involve a lot of testing and tuning to get the correct ratio of bending speed to translation speed.

4.2.4 Materials and Sanitation

Currently, the system is constructed out of fast prototyping materials such as PLA. Research will need to be done to find out what materials and manufacturing techniques can be used to be properly cleaned and sanitized after ex vivo or cadaver testing. We did not research what materials should be used in medical devices as we primarily focused on overall system integration. With the overall functionality shown to be viable, more focus can be put on improving the device to be used in a specific environment. This is part of the Technology Readiness Levels 7 and 8.

4.2.5 Steerable Sheath

We faced intermittent problems with steerable sheaths and end caps breaking when overstrained. Work could be done to reduce the force required to fully actuate the steerable sheath, and investigate why this issue occurs, in order to reduce the likelihood of failure. Perhaps refining the notch cut depth to still maintain the desired bending characteristics, while reducing the required force, would solve this issue. We also only investigated uniform notch geometry. Variable notch

size could also be investigated to cause different sections of notches to close at different rates, creating a steerable sheath that bends in a more complex curve to potentially improve reachability. More research should be done to further investigate the relationship between steerable sheath configuration and reachability. Specifically, what values of L and R are best for reachability when used by a physician in a procedure-like environment, not just in simulation.

4.3 Conclusion

Our work this year produced a prototype that is ready to be tested by laryngologists in cadavers. We met three out of four of our design goals. The steerable sheath in our design has a 1.1 mm outer diameter, and along with the spring coil tubing, fits into the 2 mm working channel of the endoscope. We are able to continuously rotate the laser fiber, satisfying our design requirement of enabling 360 degrees of rotation. We are also able to translate the laser fiber 14 mm, which achieves our design goal of being able to translate the laser fiber 1-2 cm. Lastly, we were able to bend the laser fiber 80 degrees, which falls slightly short of our goal of 90 degrees. However, we are able to bend the laser fiber in a very tight radius. The four steerable sheath designs we manufactured are able to bend in radii ranging from 3 mm to 13 mm. The geometry used in testing was 10 mm long with a 3 mm bending radius. It is possible that the laser fiber is unable to accommodate bending in such a tight radius.

We leave behind a compact, lightweight device and control panel that can be directly integrated into the existing surgical workflow. One day, a version of this device will enable physicians to treat more patients in a shorter amount of time, and treat patients who were previously considered untreatable in the office.

BIBLIOGRAPHY

- [1] J. H. Hah, S. Sim, S.-Y. An, M.-W. Sung, and H. G. Choi, "Evaluation of the prevalence of and factors associated with laryngeal diseases among the general population," *The Laryngoscope*, vol. 125, pp. 2536–2542, July 2015.
- [2] M. Remacle and H. E. Eckel, *Surgery of larynx and trachea*. Springer, 2010.
- [3] C. Y. Kuo and S. L. Halum, "Office-based laser surgery of the larynx: cost-effective treatment at the office's expense," *Otolaryngology–Head and Neck Surgery*, vol. 146, no. 5, pp. 769–773, 2012.
- [4] C. J. Rees, G. N. Postma, and J. A. Koufman, "Cost savings of unsedated office-based laser surgery for laryngeal papillomas," *Annals of Otolaryngology, Rhinology & Laryngology*, vol. 116, no. 1, pp. 45–48, 2007.
- [5] D. Stoeckel and A. Melzer, "The use of ni-ti alloys for surgical instruments," *Materials in Clinical Applications*, ed. by P. Vincenzini. Techna Srl, pp. 791–798, 1995.
- [6] K. O'Brien, Z. R. Boyer, B. G. Mart, C. T. Broliar, T. L. Carroll, and L. Fichera, "Towards flexible steerable instruments for office-based laryngeal surgery," in *2019 Design of Medical Devices Conference*, American Society of Mechanical Engineers, Apr. 2019.
- [7] J. Gafford, M. Freeman, L. Fichera, J. Noble, R. Labadie, and R. J. Webster, "Eyes in ears: a miniature steerable digital endoscope for trans-nasal diagnosis of middle ear disease," *Annals of Biomedical Engineering*, pp. 1–14, 2020.
- [8] "Office-based laryngoscopy." https://www.olympus.pl/medical/rmt/media/Content/Content-MSD/Documents/Brochures/Laryngoscopy_Manual_Prof.-Hess_15937.pdf.
Accessed: 2021-5-1.
- [9] J. Bartone, J. d'Almeida, A. Gulotta, and N. Pacheco, *SCREAM 2.0: Super-elastic Continuum Robot for Endoscopic Articulation and Manipulation*.
PhD thesis, WORCESTER POLYTECHNIC INSTITUTE, 2020.
- [10] "Online protractor." https://www.ginifab.com/feeds/angle_measurement/.
Accessed: 2021-5-5.

BIBLIOGRAPHY

- [11] S. Katsenos and H. D. Becker, "Recurrent respiratory papillomatosis: a rare chronic disease, difficult to treat, with potential to lung cancer transformation: apropos of two cases and a brief literature review," *Case reports in oncology*, vol. 4, no. 1, pp. 162–171, 2011.
- [12] I. A. Chan, J. F. d'Almeida, A. J. Chiluisa, T. L. Carroll, Y. Liu, and L. Fichera, "On the merits of using angled fiber tips in office-based laser surgery of the vocal folds," in *Medical Imaging 2021: Image-Guided Procedures, Robotic Interventions, and Modeling*, vol. 11598, p. 115981Z, International Society for Optics and Photonics, 2021.
- [13] P. J. Swaney, P. A. York, H. B. Gilbert, J. Burgner-Kahrs, and R. J. Webster, "Design, fabrication, and testing of a needle-sized wrist for surgical instruments," *Journal of Medical Devices*, vol. 11, Dec. 2016.
- [14] L. Bailly, T. Cochereau, L. Orgeas, N. H. Bernardoni, S. R. Du Roscoat, A. Mcleer-Florin, Y. Robert, X. Laval, T. Laurencin, P. Chaffanjon, *et al.*, "3d multiscale imaging of human vocal folds using synchrotron x-ray microtomography in phase retrieval mode," *Scientific reports*, vol. 8, no. 1, pp. 1–20, 2018.
- [15] "Pentax medical accessories & peripherals." <https://www.pentaxmedical.com/pentax/en/110/2/Reusable-Accessories-Autoclavable>.
Accessed: 2021-5-5.
- [16] "Dr. templeman co. small spring specialists." <http://stocksprings.drtempleman.com/viewitems/spring-guides/spring-guide>.
Accessed: 2021-5-5.
- [17] "Micro metal gearmotor hp 6v with extended motor shaft." <https://www.pololu.com/product/2218>.
Accessed: 2021-5-5.
- [18] "Technology readiness level." https://www.nasa.gov/directorates/heo/scan/engineering/technology/txt_accordion1.html.
Accessed: 2021-5-1.



APPENDIX A: AUTHORSHIP

Section	Title	Author
-	Abstract	Sabrina Liu
-	Executive Summary	Everyone
1	Introduction	Sabrina Liu
1.1	Paper Outline	Sabrina Liu
2	Design, Prototyping, Manufacturing, and Integration	Everyone
2.1	Gathering of Requirements	Sabrina Liu
2.2	Steerable Sheath Design	Phillip Abell
2.3	Selection of the Laser Fiber	Sabrina Liu
2.4	Spring Coil	Sabrina Liu
2.5	End Effector Cap	Samuel Johnson & Sabrina Liu
2.6	Actuation Unit	Zhongchuan Xu & Sabrina Liu
2.6.2	Final Actuation Unit	Zhongchuan Xu
2.7	Controller	Samuel Johnson & Sabrina Liu
3	Integration and Testing	Sabrina Liu
3.1	Integration	Sabrina Liu
3.2	Mechanical Design Evaluation	Sabrina Liu
3.2.1	Wrist Bending	Sabrina Liu
3.2.2	Translation	Sabrina Liu
3.2.3	Rotation	Sabrina Liu
3.3	ENT User Study	Sabrina Liu
4	Discussion and Future Work	Sabrina Liu

APPENDIX A. APPENDIX A: AUTHORSHIP

4.1	Advancement Over SCREAM 2.0	Sabrina Liu
4.2	Future Work	Everyone
4.2.1	User Study	Sabrina Liu
4.2.2	Actuation Unit	Sabrina Liu
4.2.3	Controlller	Sabrina Liu & Samuel Johnson
4.2.4	Materials and Sanitation	Phillip Abell
4.2.5	Steerable Sheath	Phillip Abell
4.3	Conclusion	Sabrina Liu

APPENDIX



APPENDIX B: WIRING DIAGRAM FOR CONTROL PANEL

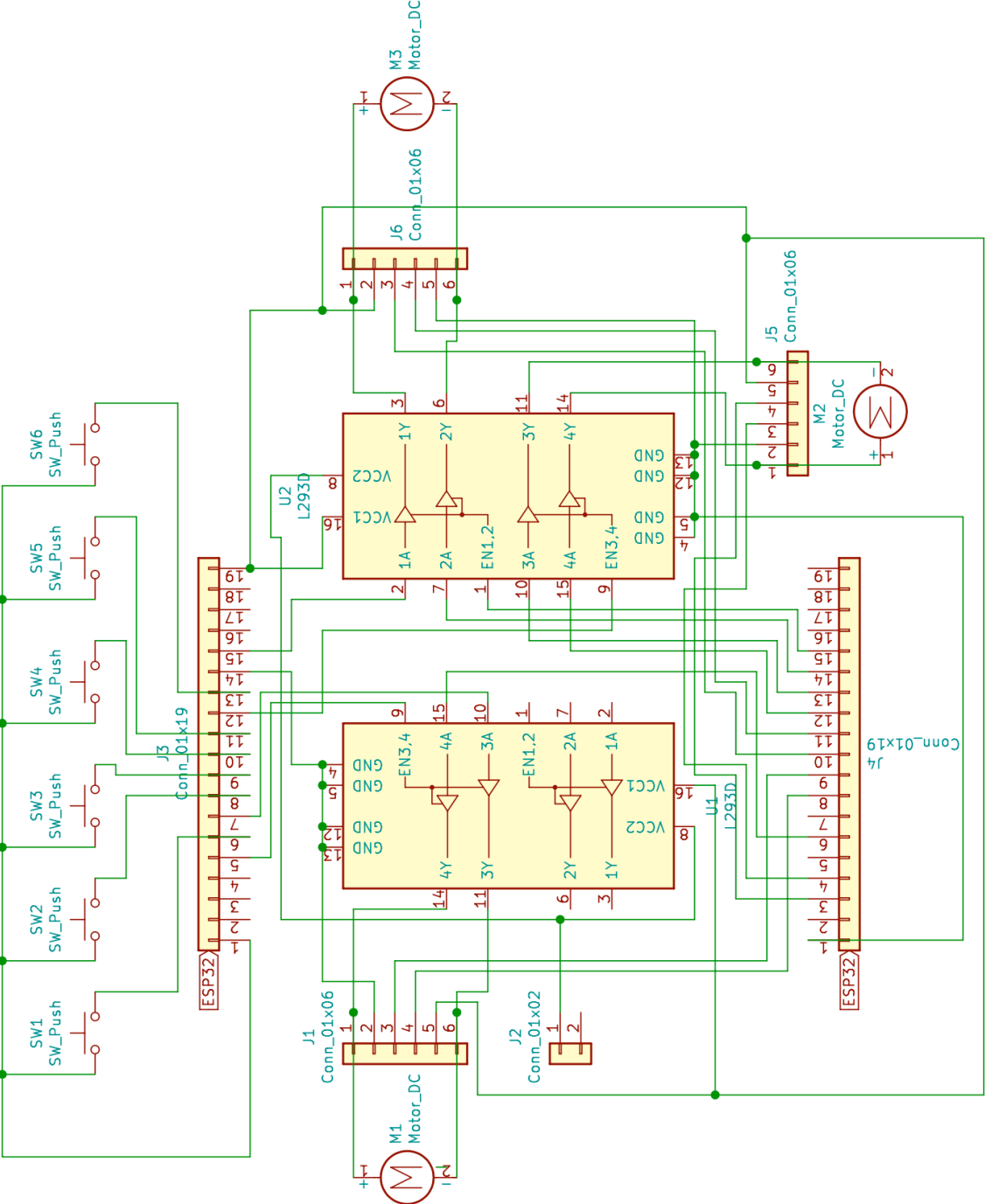


Figure B.1: Wiring diagram for button panel, H-bridges, and motors.



APPENDIX C: EXPERIMENTAL PROTOCOL FOR ENT USER STUDY

The purpose of this study is to evaluate the performance and ease of use of a miniaturized steerable optical fiber (SOF) for laser surgery of benign tumors of the voice box. The main benefit that we wish to ascertain is whether this new fiber enables more extensive anatomical access than the bare optical fibers (BOF) currently in use clinically. We ask participants to complete simulated surgical tasks in ex-vivo animal models (pig larynx). Questionnaires are distributed to study participants to understand their perceived ease of use of the device.

C.1 Overview

The simulated surgical task will be carried out using an operating endoscope (Pentax VNL-1070STK, Pentax Medical, Japan) deployed into an ex vivo porcine larynx. We had considered using a plastic anatomical manikin of a human larynx (5-Larynx and Tongue Model, Axis Scientific, USA), but plastic models are a poor substitute for actual organic tissue. We believe that using ex-vivo pig larynxes will provide a more realistic testing environment. We will ask study participants to direct the optical fiber to specific locations within the larynx, and then rate (a) how well they were able to reach the prescribed location, (b) their perceived level of comfort and mental fatigue in completing the task. We will ask participants to complete the same task twice, once with BOF, and once with the new SOF. The order in which participants will perform the two tasks will be randomized.

C.2 Experiment

Experiments will be carried out in WPI PracticePoint at 50 Prescott St., Worcester, MA 01605 and the Otolaryngology Clinic at Brigham and Women's Hospital at 45 Francis St., Boston 02115.

Study subjects will be trained ENT doctors or Senior residents (PGY4 or 5) from Boston-area hospitals who regularly perform office-based endoscopic laser treatment of laryngeal tumors. We expect to enroll between 4 and 10 subjects.

Participants will be given a 5-minute learning period to familiarize themselves with the experimental setup and the two optical fibers, i.e., the BOF and the SOF. Then, each participant will be randomly assigned to either start with the BOF or the SOF system. Participants will insert the endoscope with the laser fiber into the larynx and will be able to view the live video feed from the endoscope's chip-tip camera on a computer screen, as they would normally do during an actual procedure. The live video feed coming from the endoscope's chip-tip camera and a wide view of the workspace will be recorded for each participant, where the larynx and the participant's hands, and the endoscope are in view. Participants will be asked to maneuver the endoscope to touch the laser fiber tip to targets in the following locations:

- Left vocal fold superior surface (lowest difficulty)
- Underside/medial aspect of left vocal fold (medium difficulty)
- Juncture of 2 vocal folds in the front (anterior commissure) (medium difficulty)
- Right posterior vocal fold superior surface (high difficulty)
- Underside/medial aspect of right vocal fold (high difficulty)

After completing a set of targets, participants will take a quick survey to rate the difficulty of reaching each target with the system they are using. Then, participants will repeat the experiment with the other device. Video recordings will be taken of the live video feed from the endoscope's chip-tip camera and a wide workspace with the participant, steerable laser fiber system, and larynx setup in view. After completing both trials, participants will take a survey comparing the BOF and SOF systems.

The ex-vivo porcine larynxes will be food-grade meat handled according to appropriate safety procedures. Therefore, we do not anticipate any biohazardous exposure for participants.